Unresolved sources naturally contribute to PeV γ-ray diffuse emission observed by Tibet ASγ

Presented by: Vittoria Vecchiotti

Based on a work done in collaboration with: G. Pagliaroli, F. L. Villante, F. Zuccarini

Outline:

> **Goal:** Constrain the Galactic diffuse emission using gamma-ray observations;

1. Galactic gamma-ray diffuse emission model;
   Cataldo et al. JCAP (2019)

2. Unresolved sources *(population study of the Galactic TeV gamma-ray sources with HESS)*;
   Cataldo et al. Astrophys.J. 904 (2020)

3. Results: comparison with Tibet data and constraints on the model;
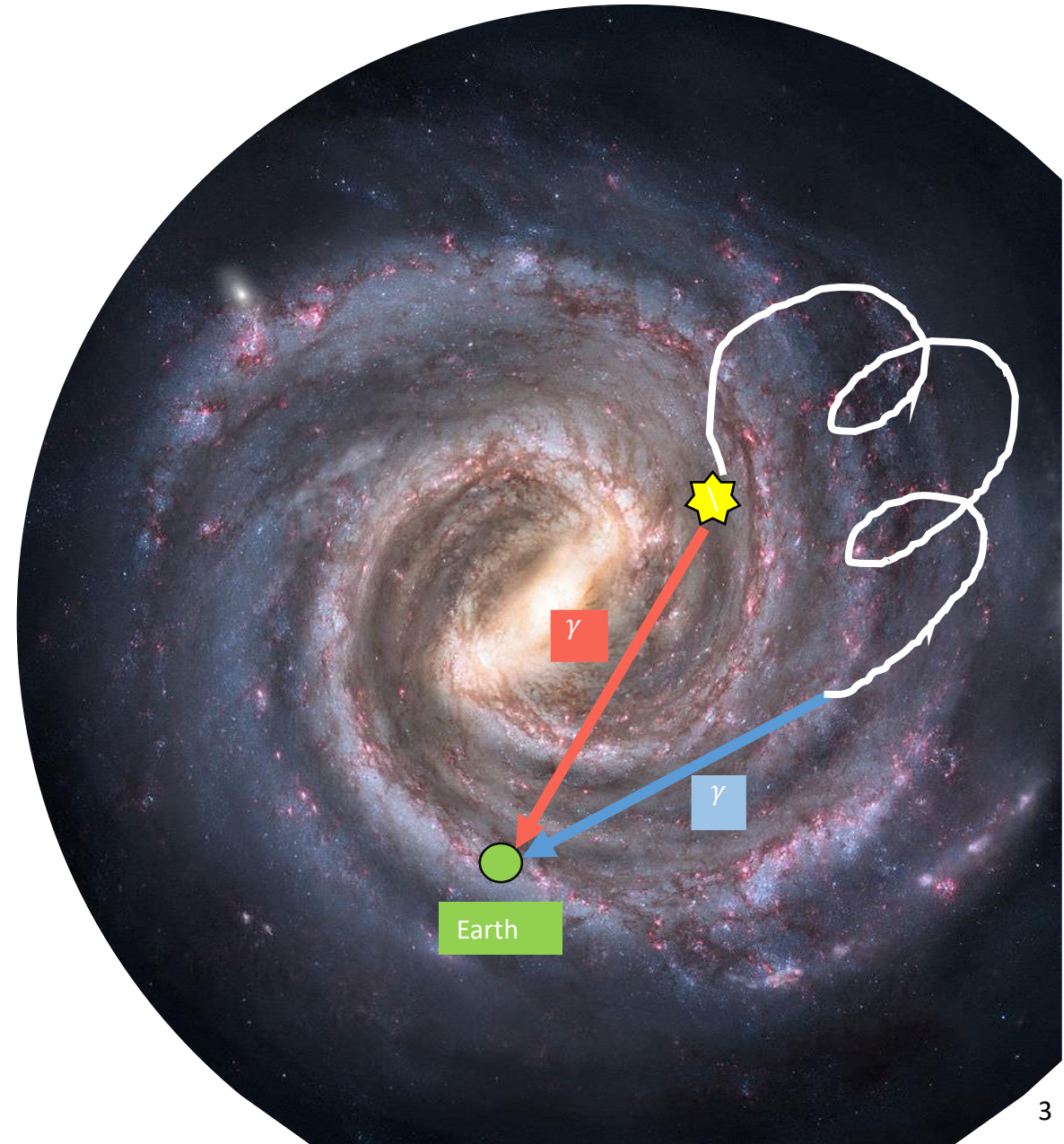   *Vecchiotti et al. Astrophys.J. (2021)*

Total Galactic emission at TeV-PeV:

$$\phi_{\gamma,tot} = \boxed{\phi_{\gamma,S}} + \boxed{\phi_{\gamma,\text{diff}}} + \cancel{\phi_{\gamma,IC}}$$

Source component is due to the interaction of accelerated particles (hadrons or leptons) with the ambient medium (ISM or CMB) within or close to an acceleration site (such as PWNe, SNRs).

Diffuse component is due to the interaction of accelerated hadrons with the interstellar medium;

Inverse Compton: is due to the interaction of accelerated leptons with the CMB ;

Total Galactic emission at TeV-PeV:

$$\phi_{\gamma,tot} = \phi_{\gamma,S} + \phi_{\gamma,\text{diff}} + \phi_{\gamma,IC}$$

Source compo...   ...raction of
accelerated ...   ...s) with the
ambient r...   ...close to an
accelera...

We want to constrain the diffuse emission

Diffuse ...   ...eraction of
accelerat...   ...edium;

Inverse Comp...   ...e interaction of
accelerated leptons ...   ...MB ;

γ

γ

Earth

4
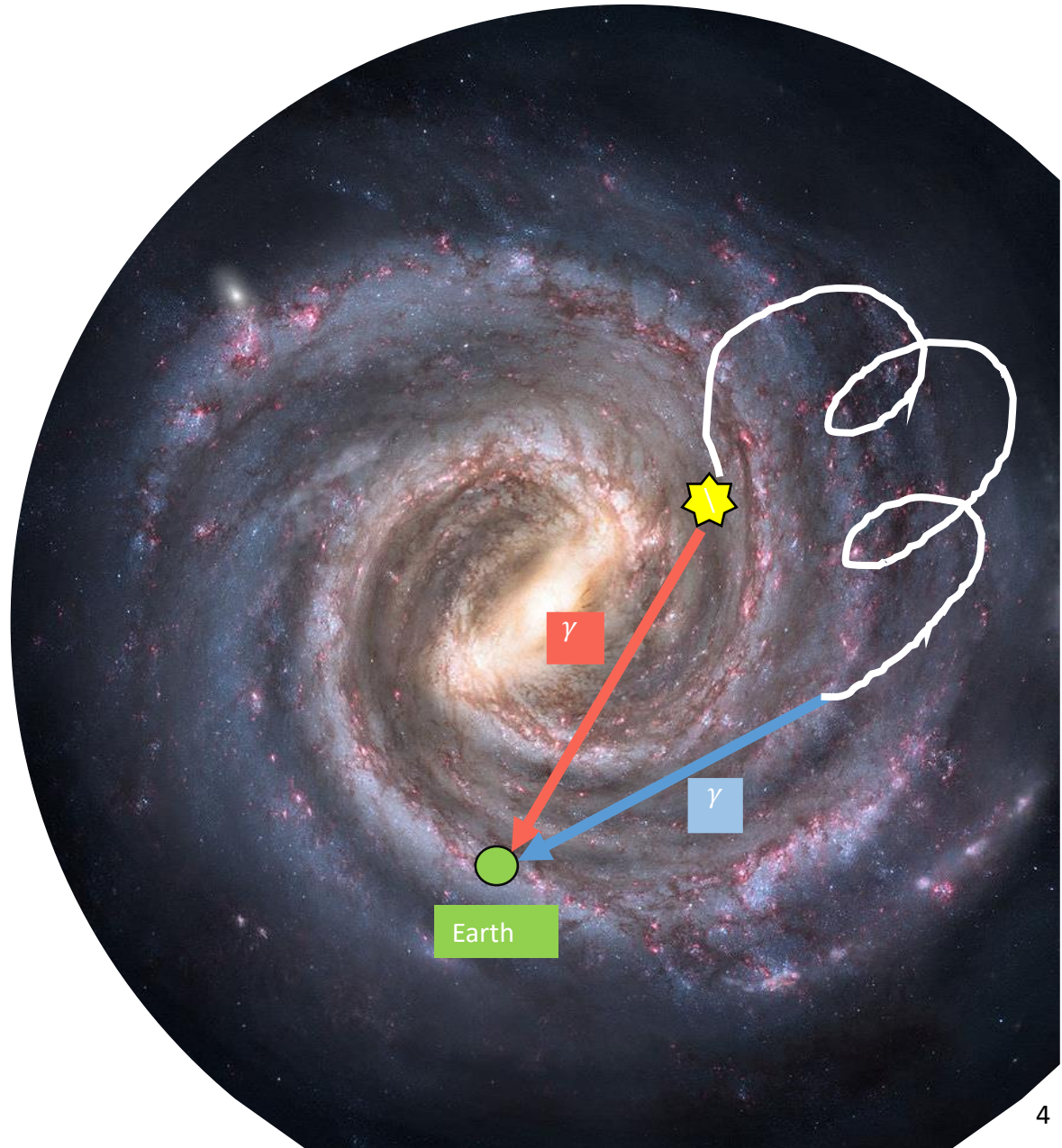
Tibet ASγ :

$$\phi_{\gamma,\text{diff}}^{Tibet}$$

First measurement of the Galactic diffuse γ-ray emission in the sub-PeV energy range.

They exclude the contribution from the known TeV sources (within 0.5 degrees) listed in the TeV source catalog.

Tibet ASγ :

$\phi_{\gamma,\mathrm{diff}}^{Tibet}$

→ First measurement of the Galactic diffuse γ-ray emission in the sub-PeV energy range.

They exclude the contribution from the known TeV sources (within 0.5 degrees) listed in the TeV source catalog.

The Tibet measurements are contaminated by the presence of Unresolved Sources

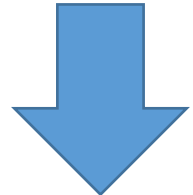$$\phi_{\gamma,\mathrm{diff}}^{Tibet} = \phi_{\gamma, S}^{UnRes} + \phi_{\gamma,\mathrm{diff}}$$

Population study
(H.E.S.S.)→ we obtain general information on the sources

Models:
Assumptions on the CR spatial and energy distributions.

6

Diffuse Galactic gamma-ray emission:

$$\phi_{\gamma,S}^{UnRes} + \phi_{\gamma,\text{diff}}$$

Interstellar gas distribution in the Galaxy [Galprop]

$$\varphi_\gamma^{diff}(E_\gamma, \hat{n}_\gamma) = \int_{E_\gamma}^\infty dE \frac{d\sigma(E, E_\gamma)}{dE_\gamma} \int_0^\infty dl \, \varphi_{CR}(E, \bar{r}_{Sun} + l\hat{n}_\gamma) \, n_H(\bar{r}_{Sun} + l\hat{n}_\gamma)$$

Differential inelastic cross section of pp interaction from the SYBILL code
[Kelner,Aharonian,Bugayov (2006)]

Cosmic-ray energy and spatial distribution

2 models for the diffuse fluxes **for 2 assumptions of the CR distribution** in the Galaxy.

Cosmic ray distribution:

$$\varphi_{CR}(E, \vec{r}) = \varphi_{CR,Sun}(E)\, g(\vec{r}, R)\, h(E, \vec{r})$$

★ Data driven local CR spectrum [*Dembinski, Engel, Fedynitch et al. (2018)*]

★ g(r) is determined by the distribution of the CR sources $f_s(\vec{r})$ (proportional to the SNR number density by Green et al. (2015), and by the propagation of CR in the Galactic magnetic field.
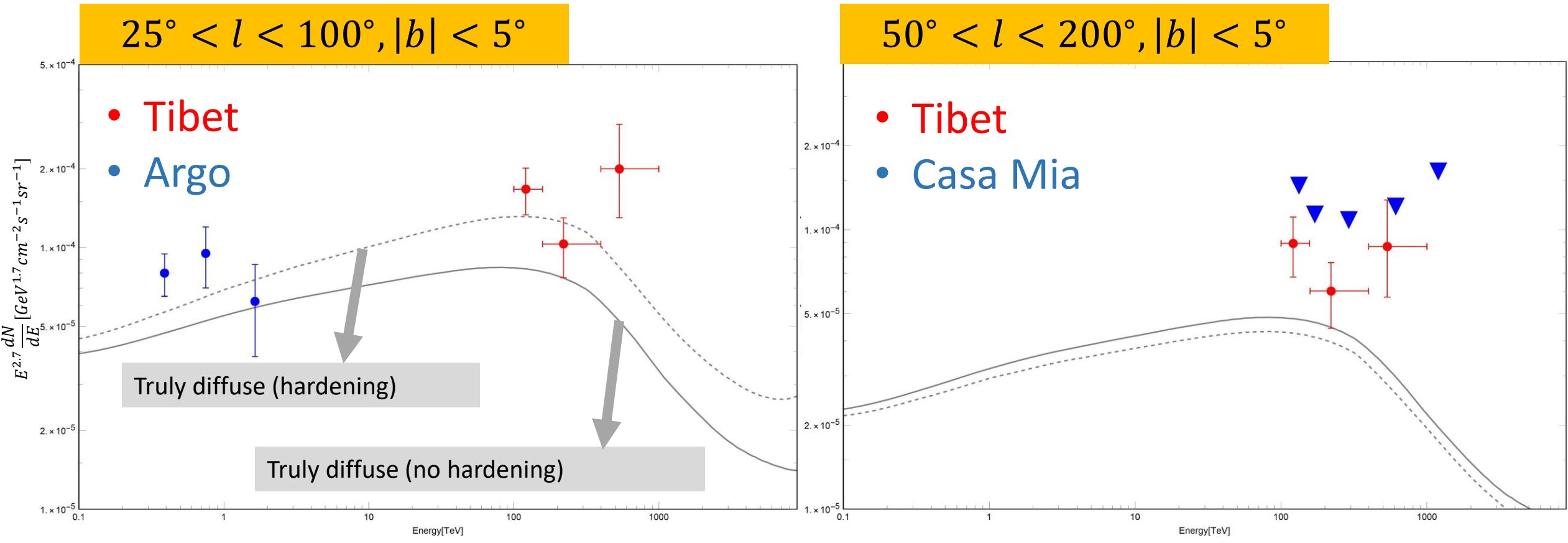
★ **2 cases: with and without spatially dependent CR spectral index**
(from the analysis of the FermiLAT data at $\sim 20\ GeV$ [*Acero et al. (2016), Yang et al. (2016), Gaggero et al. (2018)*])

$$h(E, \vec{r}) = \left(\frac{E}{20\ GeV}\right)^{\Delta(\vec{r})}$$

$$\Delta(\vec{r}, z) = 0.3\left(1 - \frac{r}{r_{sun}}\right) \text{ for } r < 10 \text{ kpc}$$
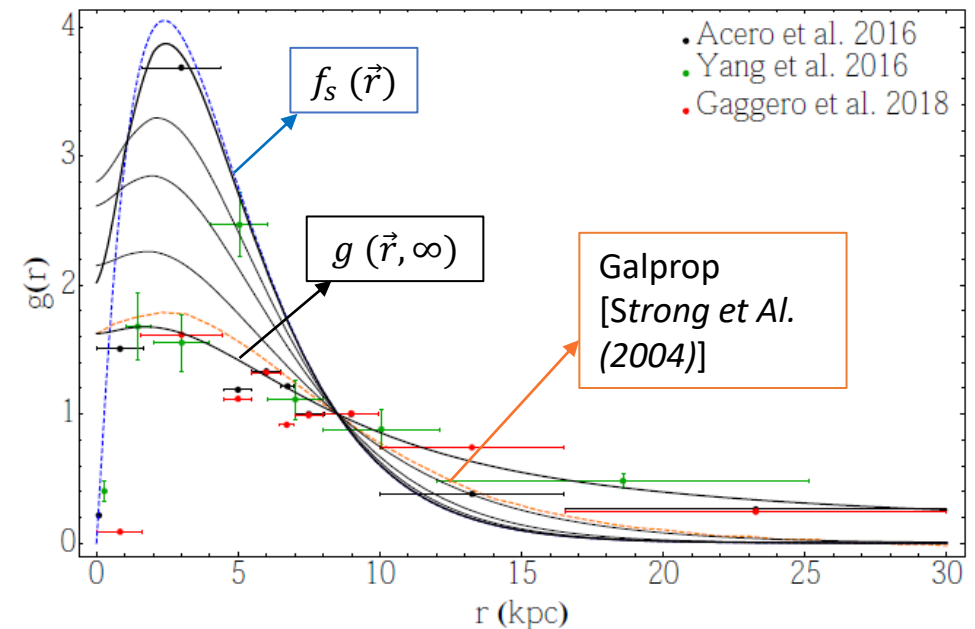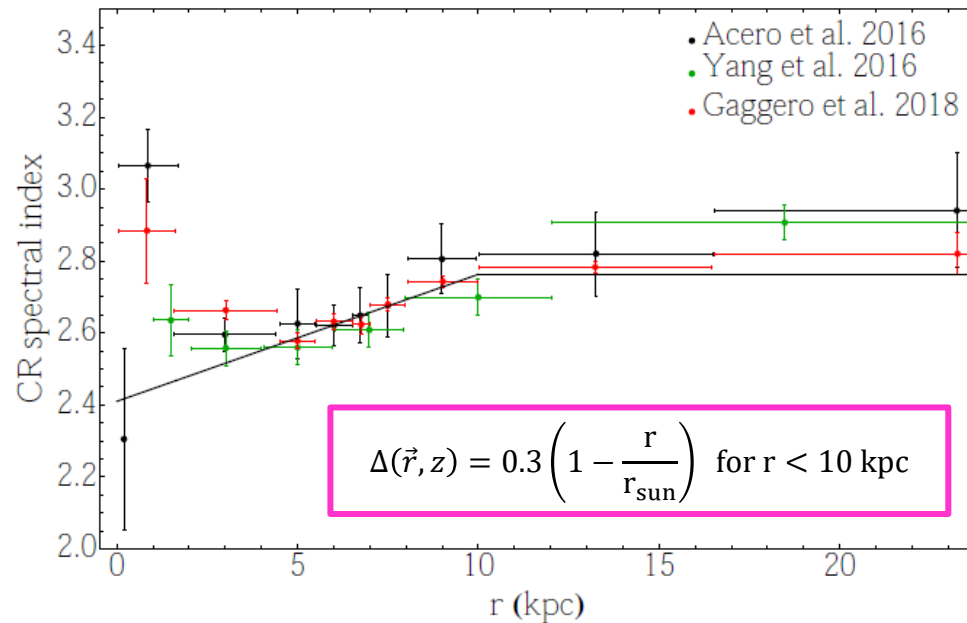
Diffuse Galactic gamma-ray emission:

Definition: Hardening ≡ spatially dependent CR spectral index

$25° < l < 100°, |b| < 5°$

- Tibet
- Argo

Truly diffuse (hardening)

Truly diffuse (no hardening)

$E^{2.7}\frac{dN}{dE}[GeV^{1.7}cm^{-2}s^{-1}sr^{-1}]$

Energy[TeV]

$50° < l < 200°, |b| < 5°$
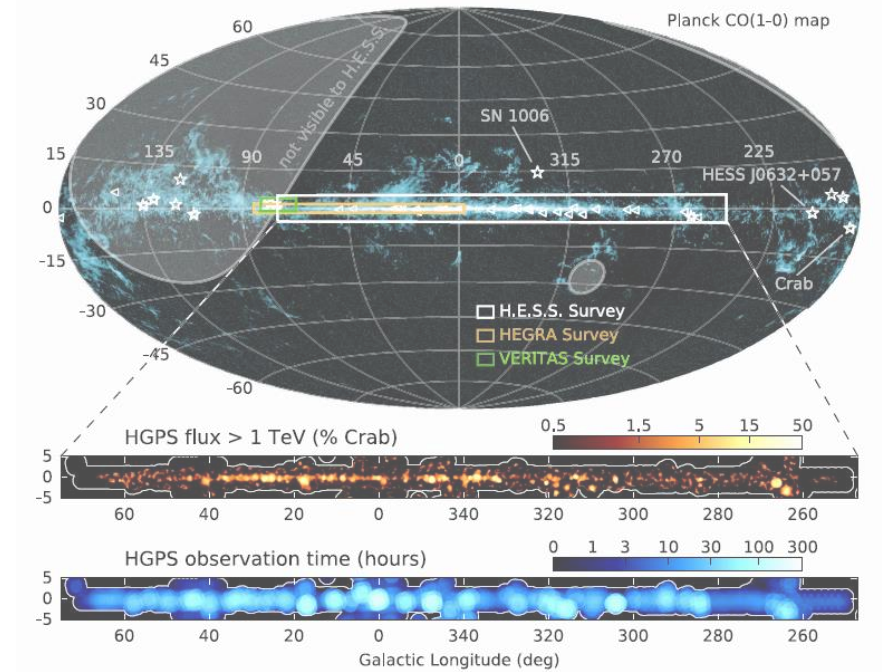
- Tibet
- Casa Mia

Energy[TeV]

Unresolved Source component:

Study of the Pulsar wind nebulae population in the TeV range:

Cataldo et al. *Astrophys.J.* 904 (2020)

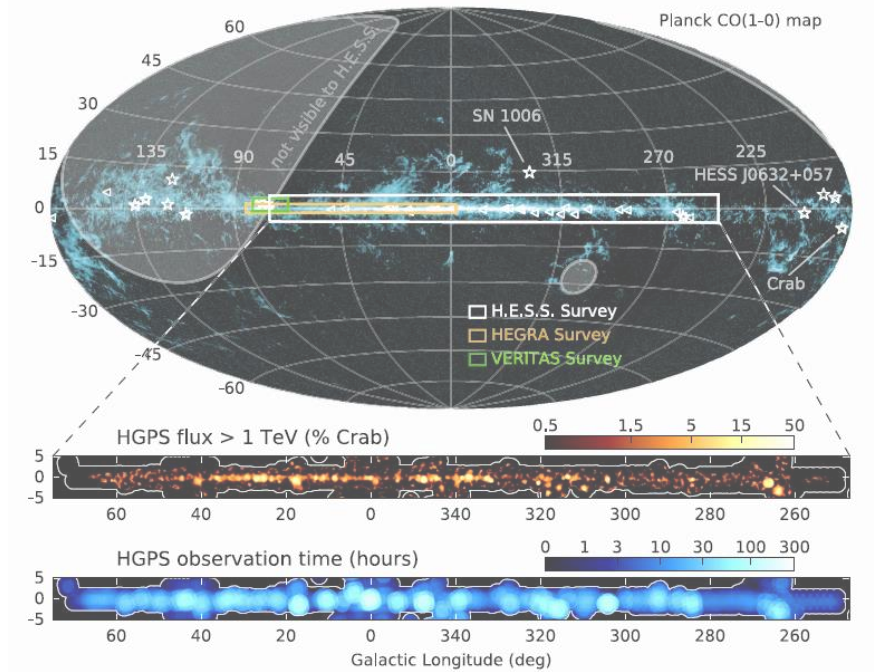- The HGPS catalogue ($\phi > 0.1\phi_{Crab}$);

Unresolved Source component:

Study of the Pulsar wind nebulae population in the TeV range:

Cataldo et al. *Astrophys.J.* 904 (2020)

- The HGPS catalogue ($\phi > 0.1\phi_{Crab}$);

- Model for TeV source population:
  we assume the spatial distribution and the
  luminosity distribution of the sources;

$$\frac{dN}{d^3rdL} = \rho(r)Y(L)$$
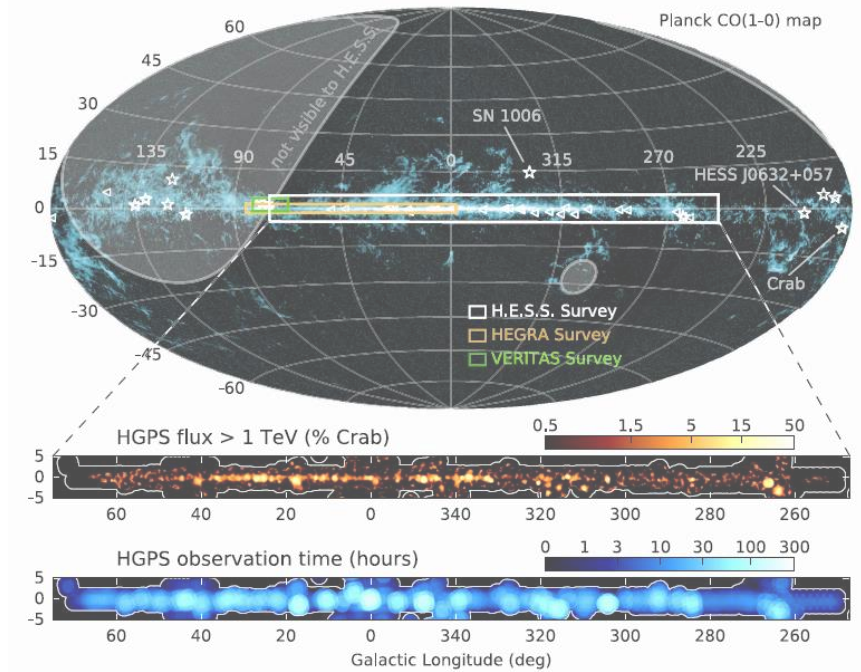
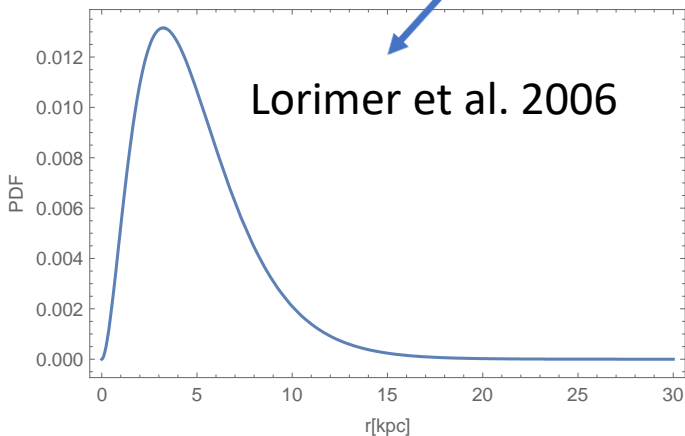**Abdalla et al, *A&A*, 612, A1 (2018)**

11

Unresolved Source component:

Study of the Pulsar wind nebulae population in the TeV range:

Cataldo et al. *Astrophys.J.* 904 (2020)

- The HGPS catalogue ($\phi > 0.1\phi_{Crab}$);

- Model for TeV source population:
  we assume the spatial distribution and the
  luminosity distribution of the sources;

$$\frac{dN}{d^3rdL} = \rho(r)Y(L)$$

Lorimer et al. 2006

Unresolved Source component:

Study of the Pulsar wind nebulae population in the TeV range:

Cataldo et al. *Astrophys.J.* 904 (2020)

- The HGPS catalogue ($\phi > 0.1 \phi_{Crab}$);

- Model for TeV source population:
  we assume the spatial distribution and the
  luminosity distribution of the sources;
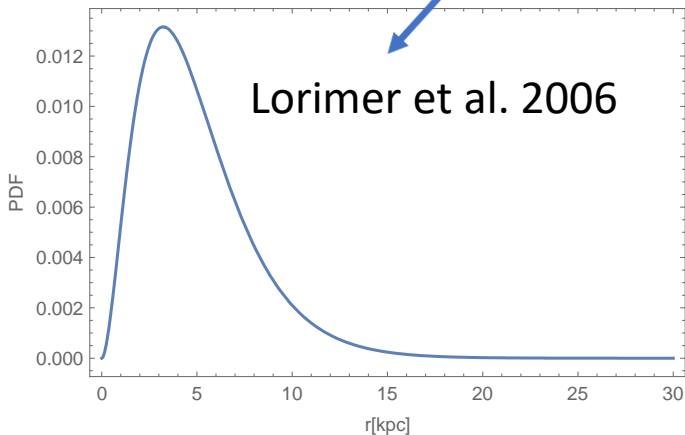
$$\frac{dN}{d^3 r dL} = \rho(r) Y(L)$$

$$Y(L) = \frac{R \tau (\alpha - 1)}{L_{\max}} \left(\frac{L}{L_{\max}} \right)^{-\alpha}$$

Lorimer et al. 2006

$$\alpha = 1/\gamma + 1$$

$$R = 0.019 \,\mathrm{yr}^{-1}$$

For pulsar-powered sources:

$$L(t) = L_{\max} \left(1 + \frac{t}{\tau} \right)^{-\gamma}$$

Unresolved Source component:

Study of the Pulsar wind nebulae population in the TeV range:

Cataldo et al. *Astrophys.J.* 904 (2020)

- The HGPS catalogue ($\phi > 0.1\phi_{Crab}$);

- Model for TeV source population:
  we assume the spatial distribution and the
  luminosity distribution of the sources;
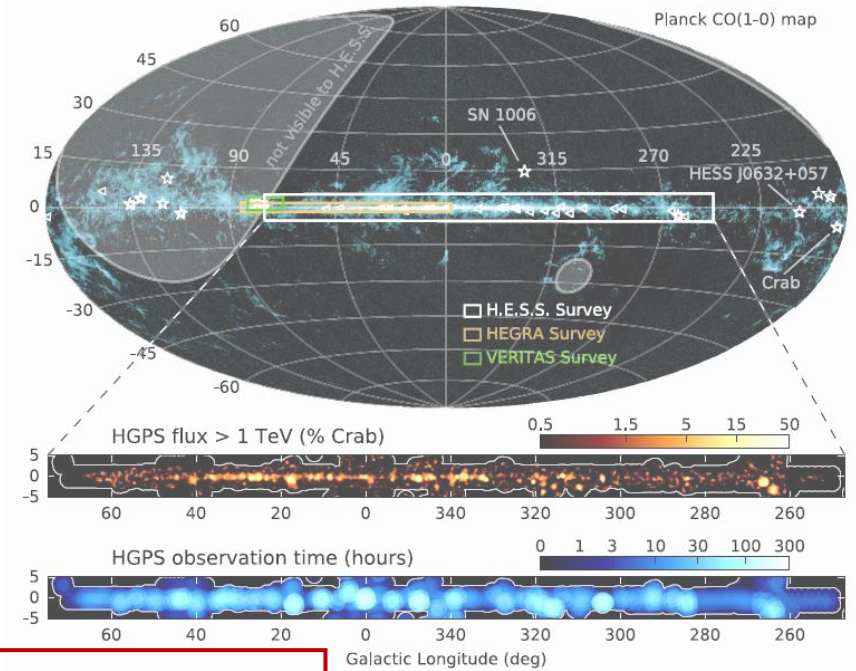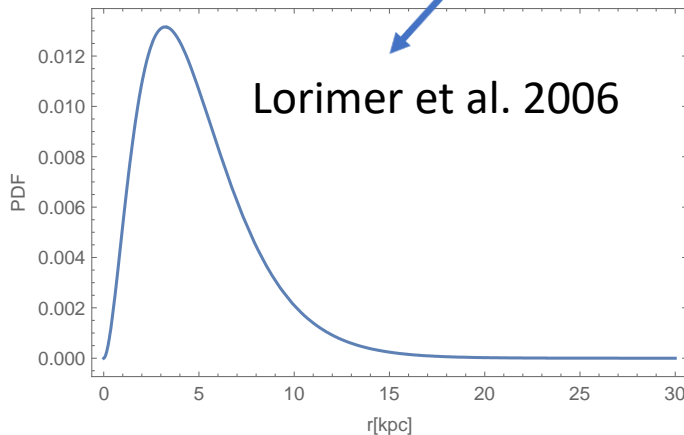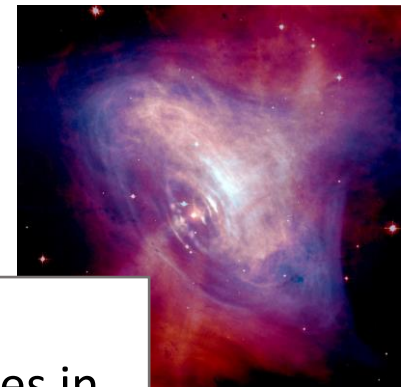
$$\frac{dN}{d^3r\,dL} = \rho(r)Y(L)$$

$$Y(L) = \frac{R\,\tau\,(\alpha - 1)}{L_{\max}}\left(\frac{L}{L_{\max}}\right)^{-\alpha}$$

Lorimer et al. 2006

$$\alpha = 1/\gamma + 1 \qquad \text{For pulsar-powered sources:}$$

$$R = 0.019\,\mathrm{yr}^{-1} \qquad L(t) = L_{\max}\left(1 + \frac{t}{\tau}\right)^{-\gamma}$$

We assume a **power-law** energy spectrum with index
$\boldsymbol{\beta_{TeV} = 2.3}$ that is the average index for all the sources in the HGPS catalogue.

14

Unresolved Source component:

Study of the Pulsar wind nebulae population in the TeV range:

Cataldo et al. _Astrophys.J._ 904 (2020)

We fit the H.G.P.S. catalogue with an unbinned likelihood

$$L_{max} = L^{BF}$$
$$\tau = \tau^{BF}$$

$$\Phi_{1-100\,TeV}^{tot}$$

$\alpha = 1.8$

$$L_{max} = 6.8 \times 10^{35}\ erg\ s^{-1}$$
$$\tau = 0.5\ kyr$$

$\alpha = 1.5$

$$L_{max} = 5.0 \times 10^{35}\ erg\ s^{-1}$$
$$\tau = 1.7\ kyr$$

All sources are resolved

$\alpha = 1.8$
$\alpha = 1.5$

$\beta_{\text{TeV}} = 2.3$

#Sources >Flux

Flux>1 TeV(% Crab)

Unresolved Source component:

Study of the Pulsar wind nebulae population in the TeV range:

Cataldo et al. *Astrophys.J.* 904 (2020)

We fit the H.G.P.S. catalogue with an unbinned likelihood

$$L_{max} = L^{BF}$$
$$\tau = \tau^{BF}$$

$$\Phi^{tot}_{1-100\,TeV}$$

Unresolved Sources:
$$\Phi^{unr}_{1-100\,TeV}$$

$\alpha = 1.5$

$$L_{max} = 5.0 \times 10^{35}\, erg\, s^{-1}$$

$$\tau = 1.7\, kyr$$

All sources are resolved

$\alpha = 1.8$

$\alpha = 1.5$

$\beta_{\text{TeV}} = 2.3$

#Sources >Flux

Flux>1 TeV(% Crab)

Unresolved Source component:

We have $\Phi_{1-100\,TeV}$ ➔ we need $\phi(E)$:

- Spectral assumption: power-law with an exponential cut-off.

$$\varphi(E) = \left(\frac{E}{1\,TeV}\right)^{-\beta_{TeV}} Exp\left(-\frac{E}{E_{cut}}\right)$$

$\beta_{TeV} = 2.3$ from the HGPS catalogue;

Unresolved Source component:

We have $\Phi_{1-100\ TeV}$ ➔ we need $\phi(E)$:

- Spectral assumption: power-law with an exponential cut-off.

$$\varphi(E) = \left(\frac{E}{1\ TeV}\right)^{-\beta_{TeV}} Exp\left(-\frac{E}{E_{cut}}\right)$$

$\beta_{TeV} = 2.3$ from the HGPS catalogue;

$E_{cut} = 500\ TeV$ still not well constrained but motivated by recent observations of Tibet, HAWC and LHAASO;

Amenomori, M., Bao, Y. W., Bi, X. J., et al. 2019, Phys.323Rev. Lett., 123, 051101

Abeysekara, A., Albert, A., Alfaro, R., et al. 2020, Physical316Review Letters, 124

Cao, Z., Aharonian, F. A., An, Q., et al. 2021, Nature, 594,33033

Unresolved Source component:

We have $\Phi_{1-100\ TeV}$ → we need $\phi(E)$:

- Spectral assumption: power-law with an exponential cut-off.

$$\varphi(E) = \left(\frac{E}{1\ TeV}\right)^{-\beta_{TeV}} Exp\left(-\frac{E}{E_{cut}}\right)$$

$\beta_{TeV} = 2.3$ from the HGPS catalogue;

$E_{cut} = 500\ TeV$ still not well constrained but motivated by recent observations of Tibet, HAWC and LHAASO;

Amenomori, M., Bao, Y. W., Bi, X. J., et al. 2019, Phys.323Rev. Lett., 123, 051101

Abeysekara, A., Albert, A., Alfaro, R., et al. 2020, Physical316Review Letters, 124

Cao, Z., Aharonian, F. A., An, Q., et al. 2021, Nature, 594,33033

We introduce a flux detection threshold based on the performance of H.E.S.S.
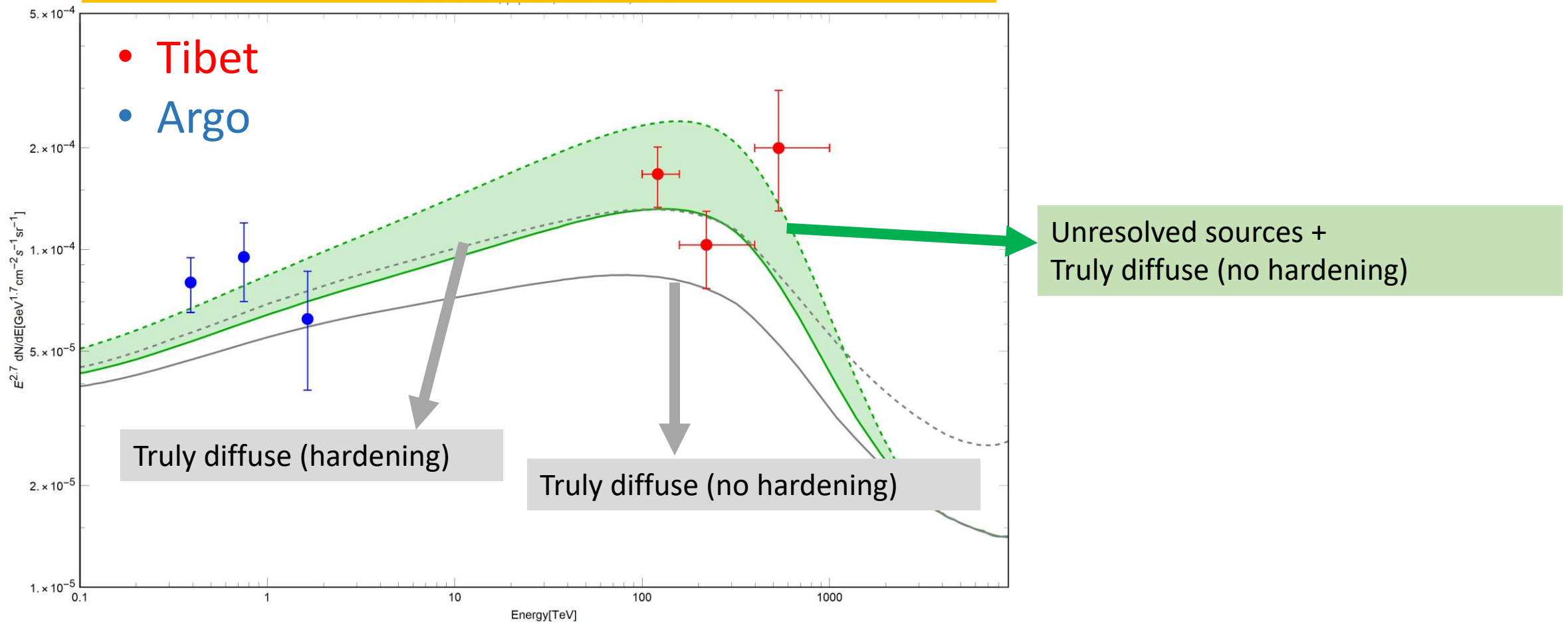$$\phi_{th} = 0.01\phi_{crab} - 0.1\phi_{crab}$$

We calculate the unresolved source contribution.

Tibet ASγ :

We add the contribution of unresolved sources to the truly diffuse emission without the hypothesis of CR spectral hardening.

Tibet ASγ : We add the contribution of unresolved sources to the truly diffuse emission without the hypothesis of CR spectral hardening.

Definition: Hardening ≡ spatially dependent CR spectral index

$$25° < l < 100°, |b| < 5°, E_{cut} = 500\ TeV$$

- Tibet
- Argo

Unresolved sources +
Truly diffuse (no hardening)

Truly diffuse (hardening)

Truly diffuse (no hardening)

21

Tibet ASγ : We add the contribution of unresolved sources to the truly diffuse emission without the hypothesis of CR spectral hardening.

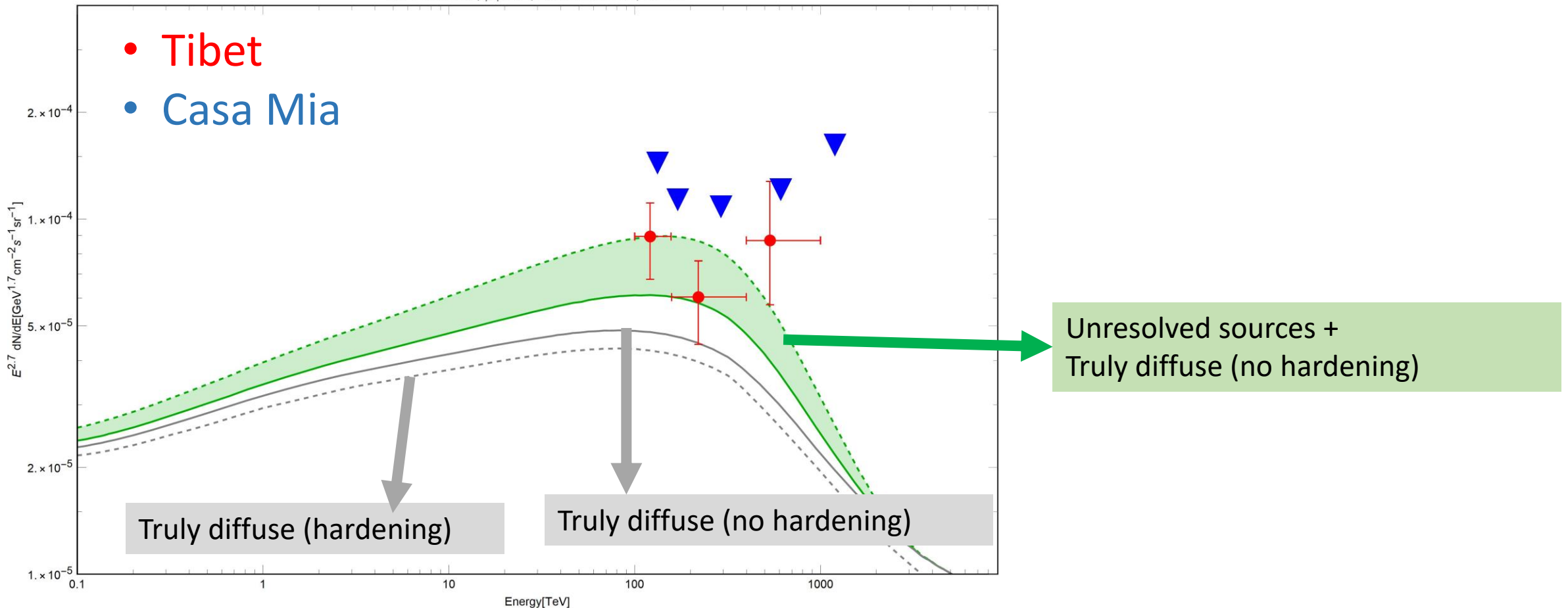*Definition: Hardening ≡ spatially dependent CR spectral index*

$$50° < l < 200°, |b| < 5°, E_{cut} = 500\ TeV$$

- **Tibet**
- **Casa Mia**

Unresolved sources +
Truly diffuse (no hardening)

Truly diffuse (hardening)

Truly diffuse (no hardening)

Summary:

- We modeled the gamma diffuse emission. We considered two different hypotheses for the CR distribution (with and without spectral hardening);
- We calculate the unresolved component from the H.E.S.S. observations.
- In the **sub-PeV** energy range the inclusion of the **unresolved PWNe** contribution produces a better description of the Tibet data than CR spectral hardening;

Looking at different sky regions is fundamental because it allows us to distinguish between the two effects.

Backup slides

Typical age of the sources:
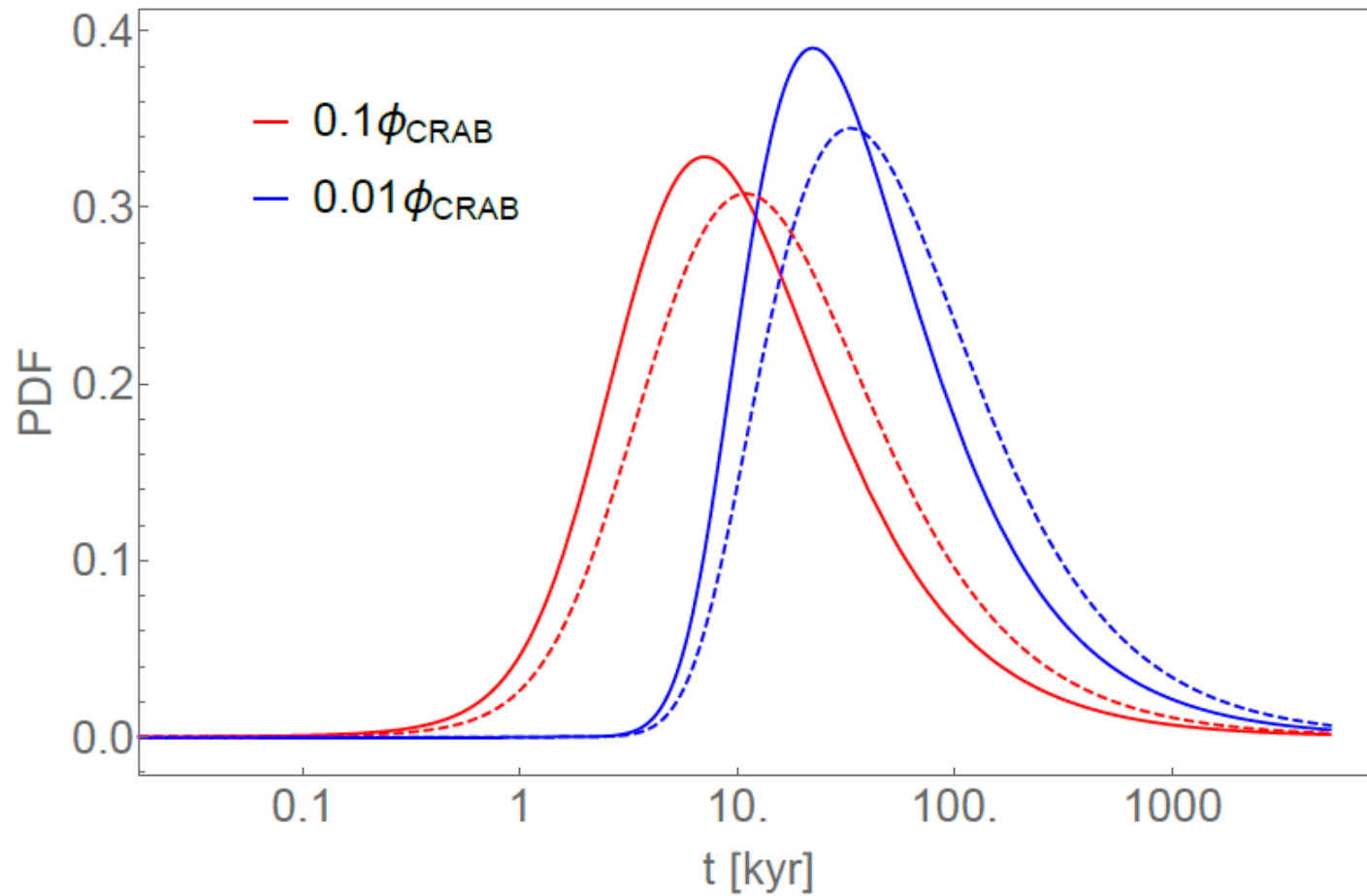
$$25° < l < 100°, |b| < 5°$$

$$50° < l < 200°, |b| < 5°$$

$$t_{age} \sim 7 - 33 \; kyr$$

How many sources will CTA be able to resolve?
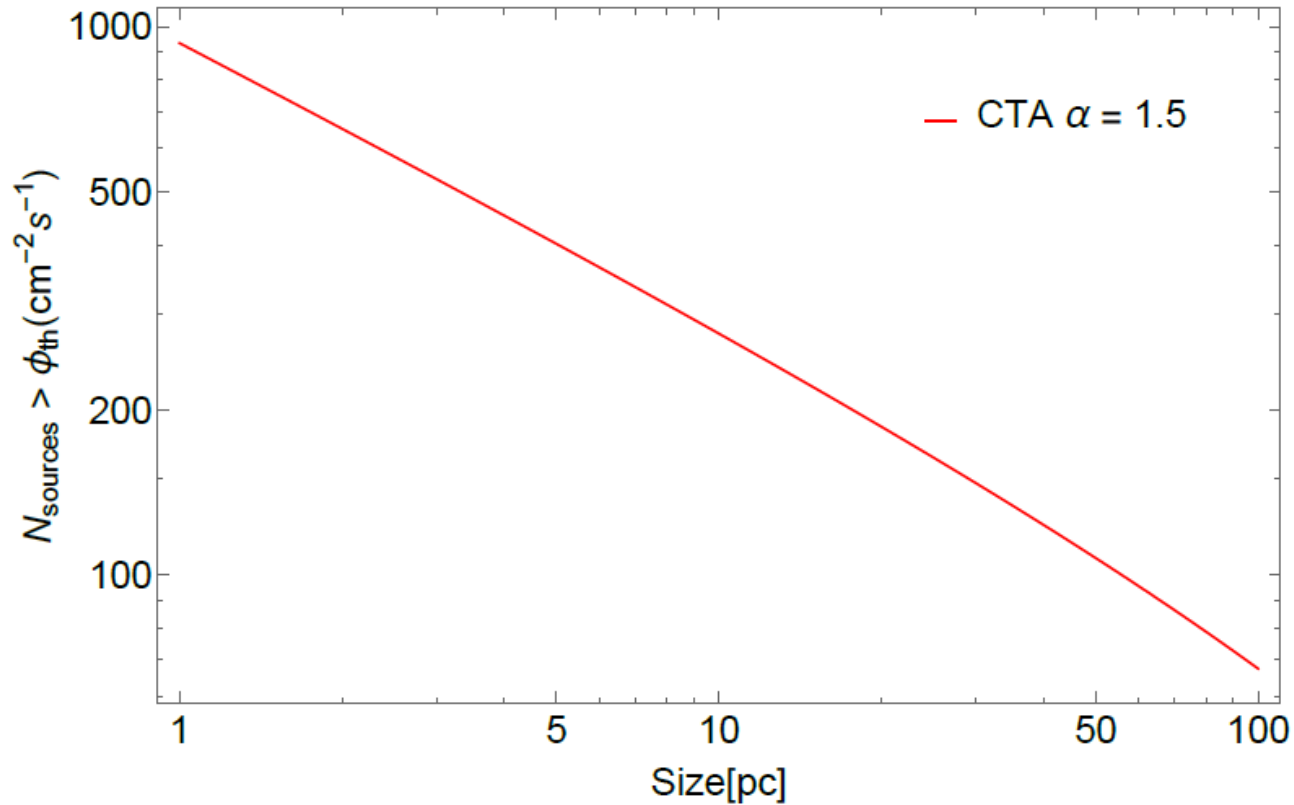
$$\phi_{th} \sim \phi_{th,ps} \frac{\theta_S}{\theta_{PSF}}$$

$$\phi_{th,ps} = 3 \times 10^{-3} \phi_{CRAB}$$

$$\theta_{PSF} = 0.05^o$$

$$280(10\ pc) - 140(40 pc)$$

Lipari and Vernetto Diffuse model:

Energy cut effect:

$$25° < l < 100°, |b| < 5°$$
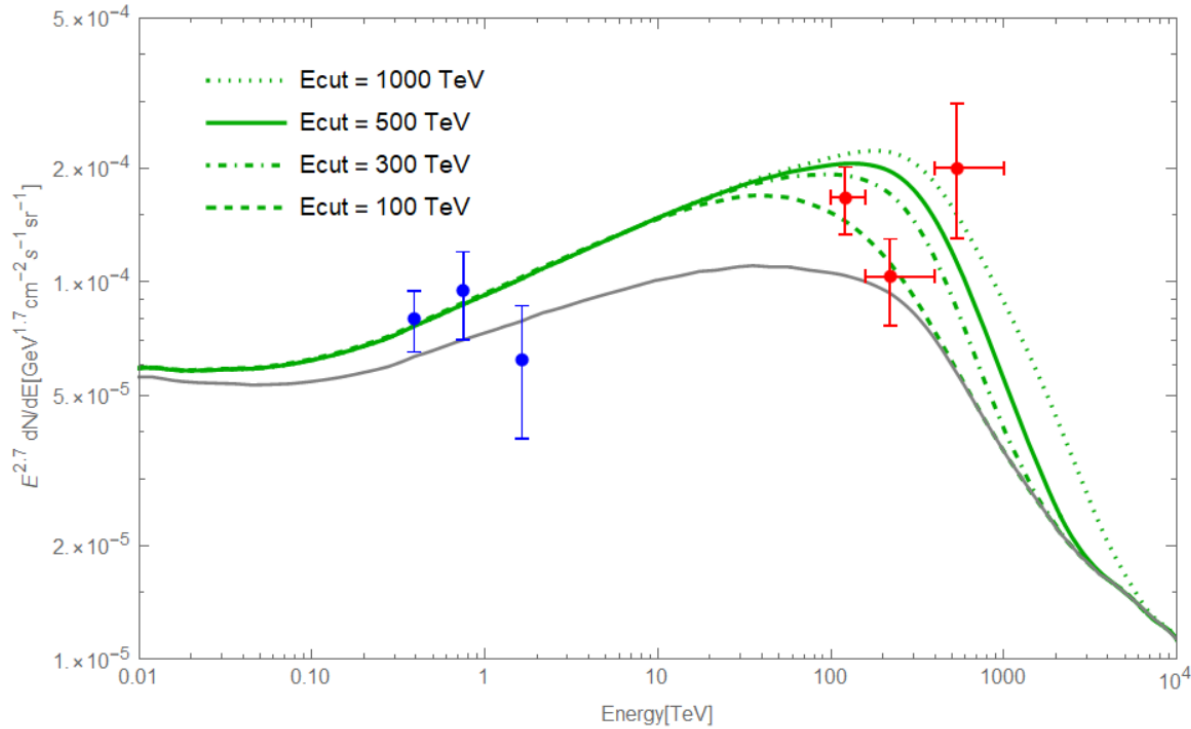
$$50° < l < 200°, |b| < 5°$$

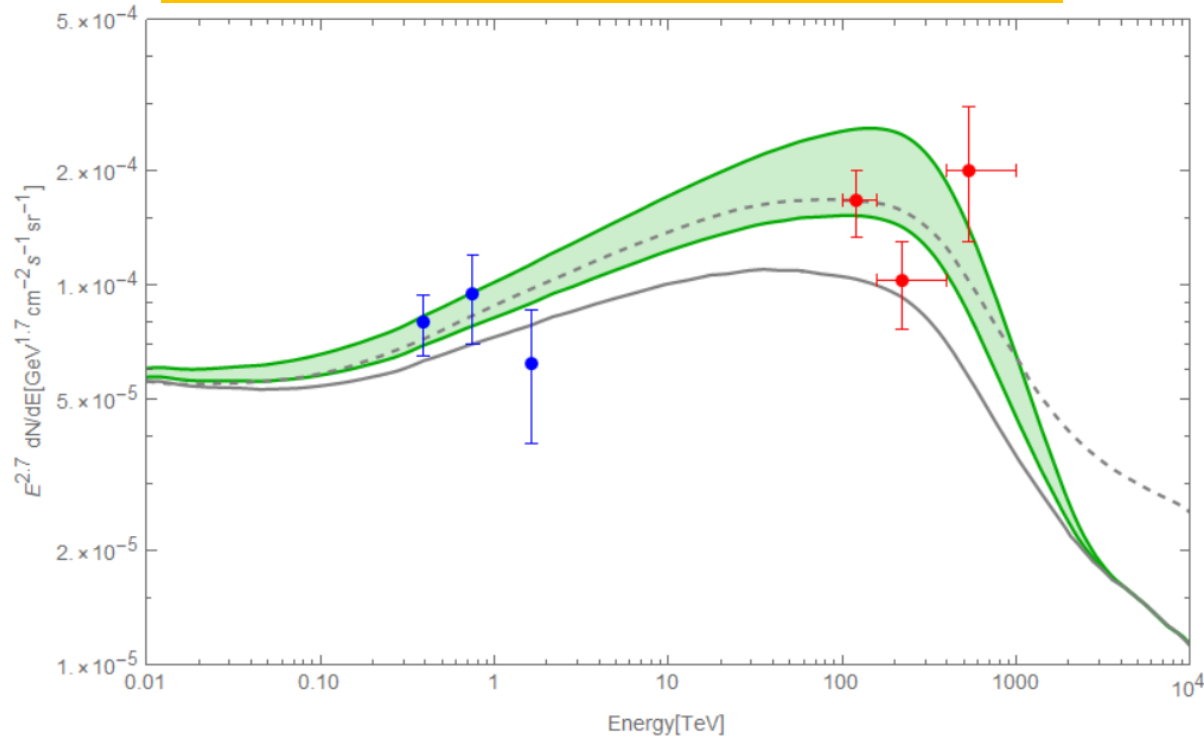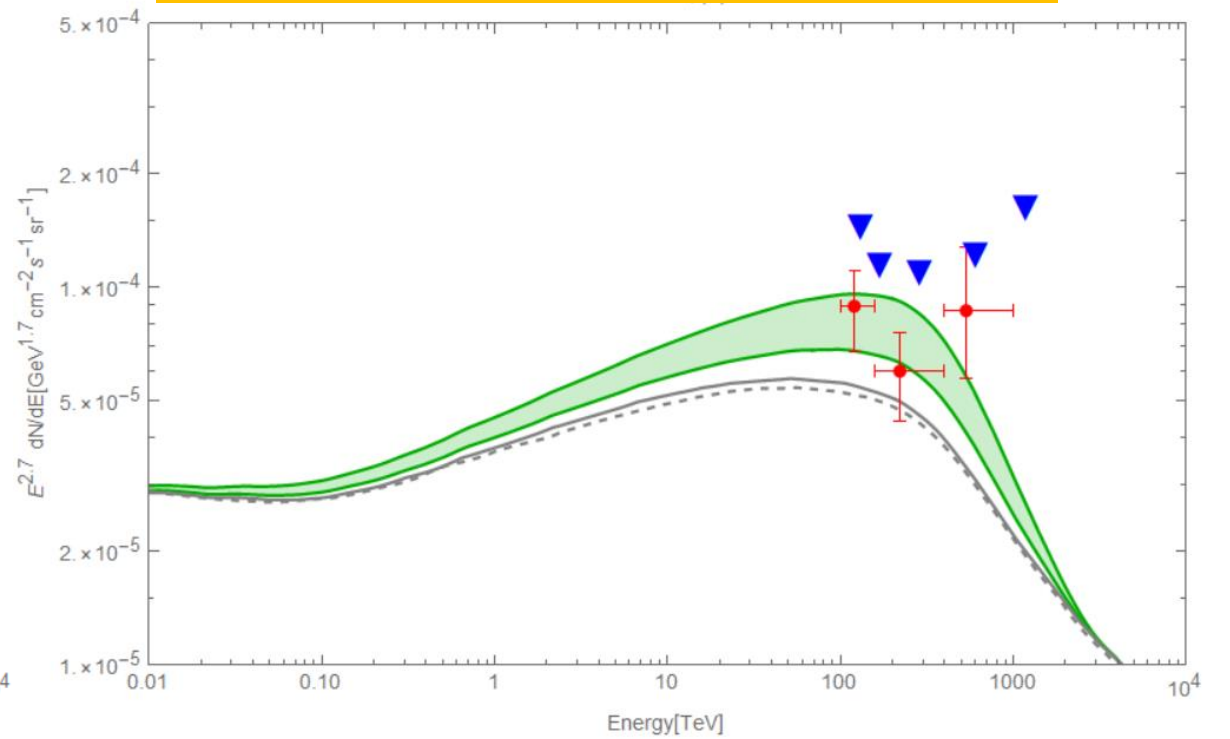# Absorption in the Sub PeV energy range:

The pair production cross section:

$$\sigma_{\gamma\gamma} = \sigma_T \left(\frac{3}{16}\right)(1-\beta^2)\left[2\beta(\beta^2-2)+(3-\beta^4)\ln\left(\frac{1+\beta}{1-\beta}\right)\right]$$

Where: $\beta = \sqrt{1-\frac{1}{x}}$ and $x = \frac{2E_\gamma\epsilon(1-\cos\theta)}{4\,m_e^2}, \ x > 1$

For a fixed values of ϵ the energy threshold is:

$$E_\gamma^{th} = \frac{2\,m_e^2}{\epsilon(1-cos\theta)} \simeq \frac{0.52}{\epsilon_{eV}(1-cos\theta)}TeV$$

The absorption probability per unit path length (for CMB) is:

$$\kappa(E_\gamma) = \int \epsilon \int d\Omega(1-\cos(\theta))n_{\gamma,CMB}(\epsilon)\sigma_{\gamma\gamma}(x(E_\gamma,\epsilon,\theta))$$

The optical depth is:

$$\tau(E_\gamma,r) = \int_0^r dr'\ \kappa(E_\gamma)$$

29
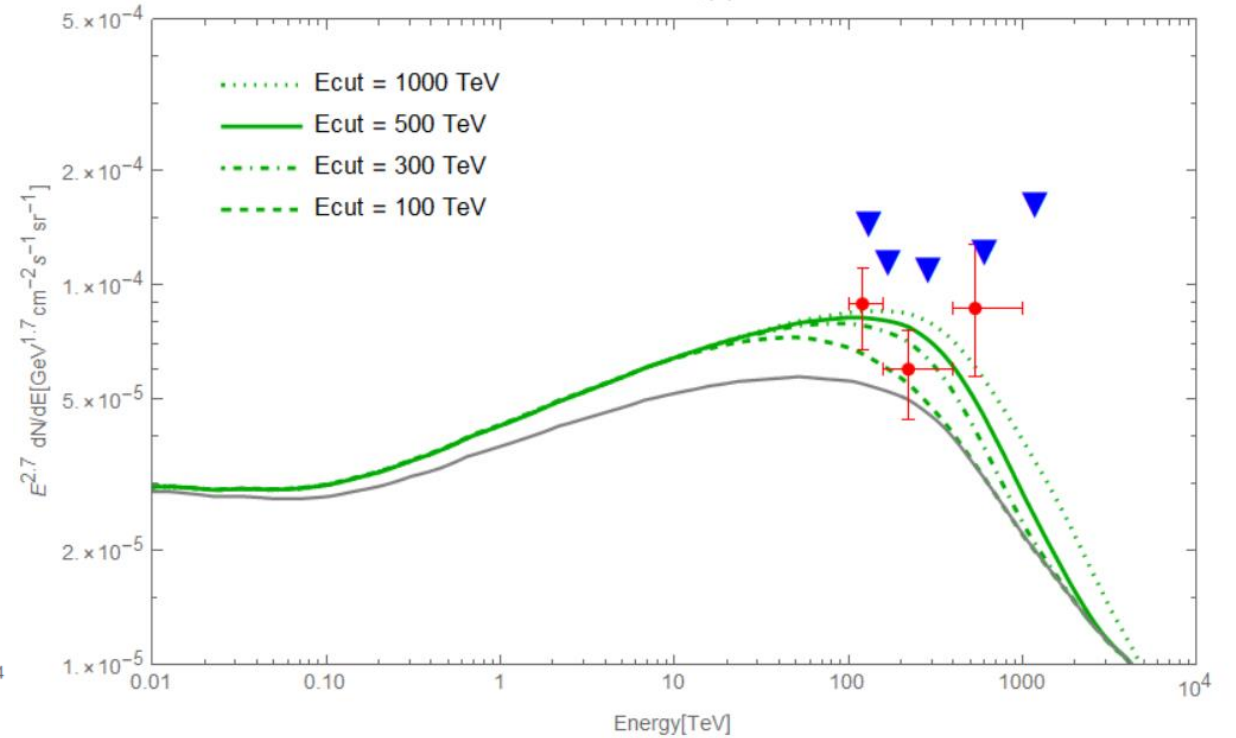
Absorption in the Sub PeV energy range:
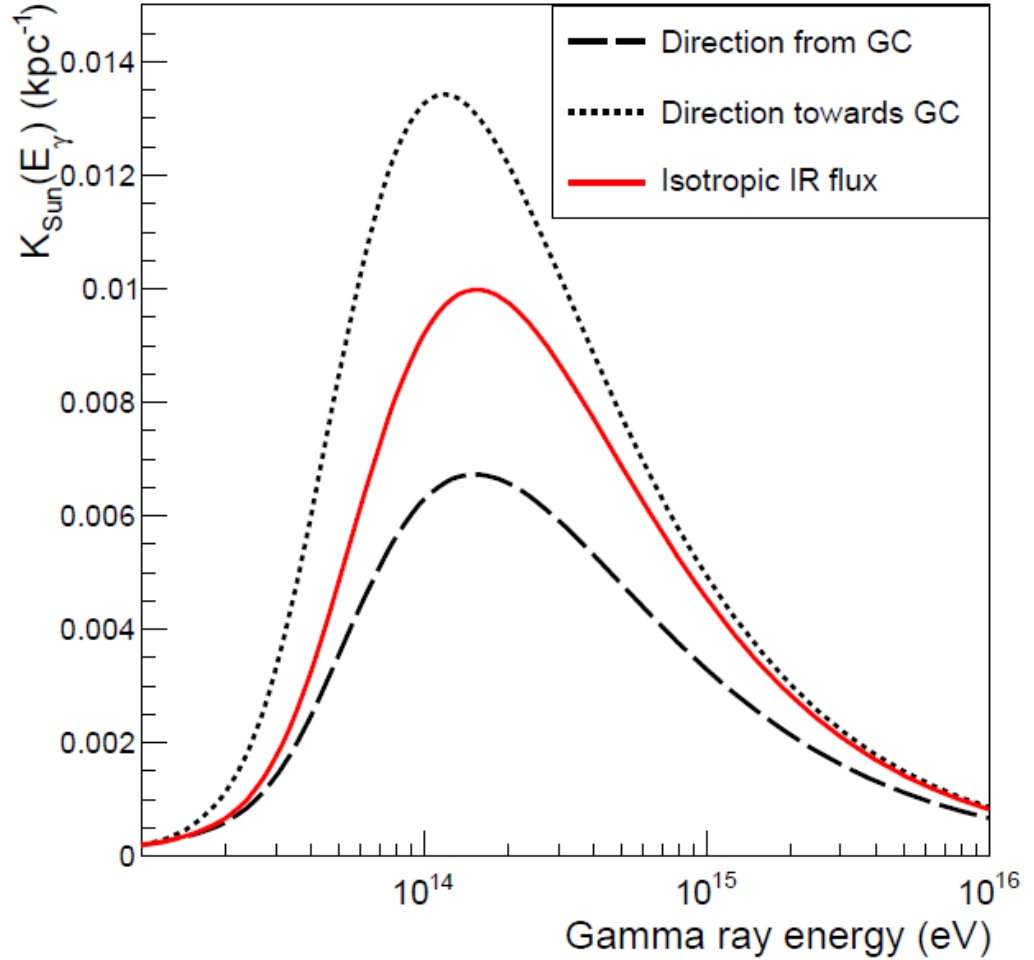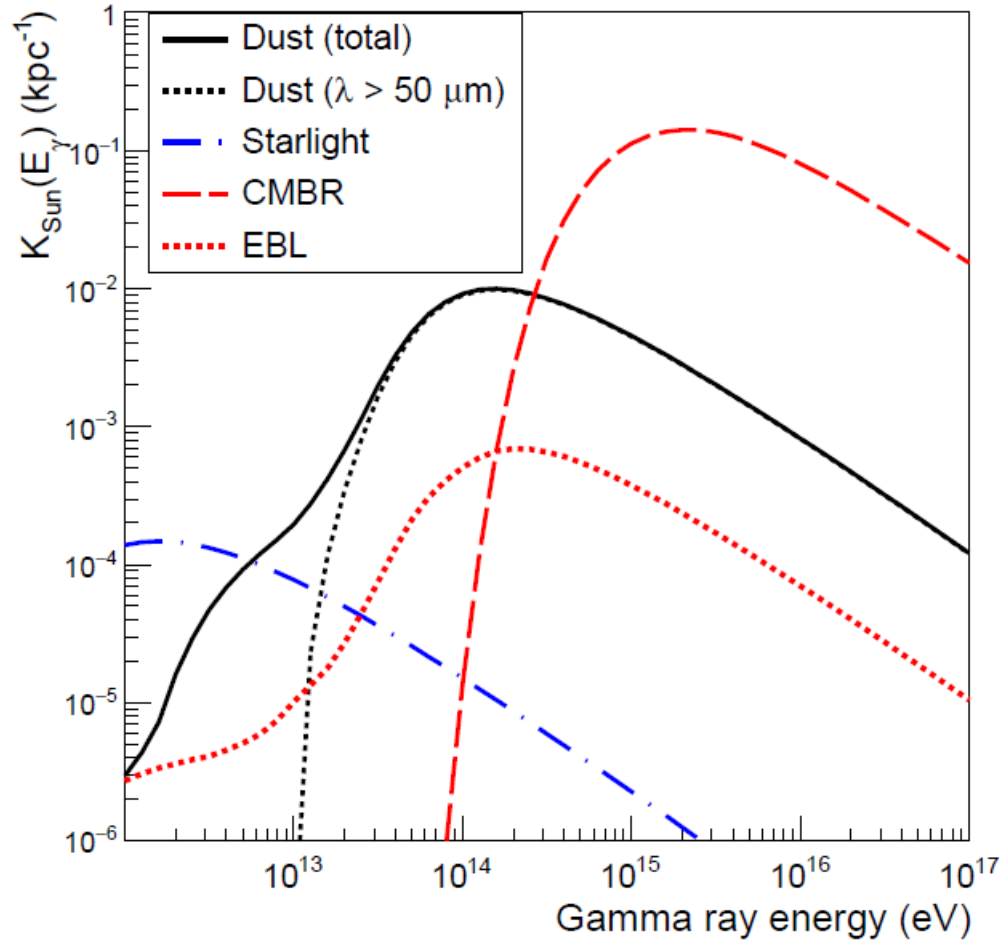
**Vernetto and Lipari, Phys. Rev. D 94, 063009
– Published 19 September 2016**

30

Comparison Diffuse models:
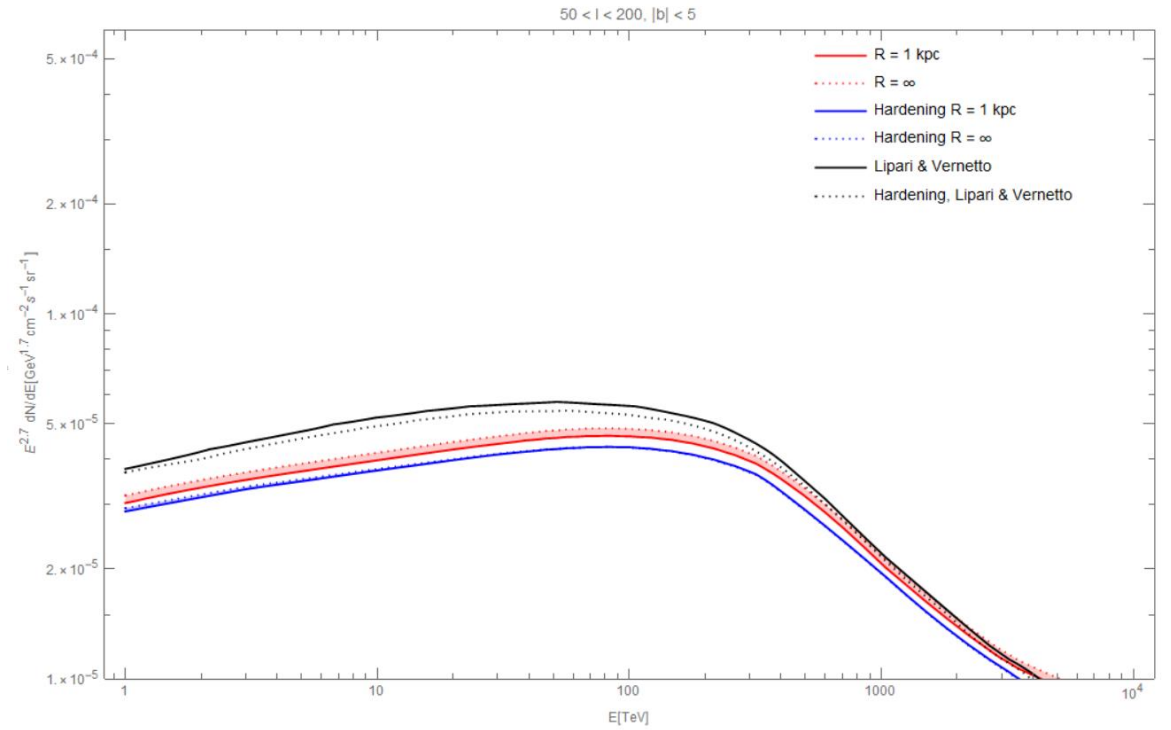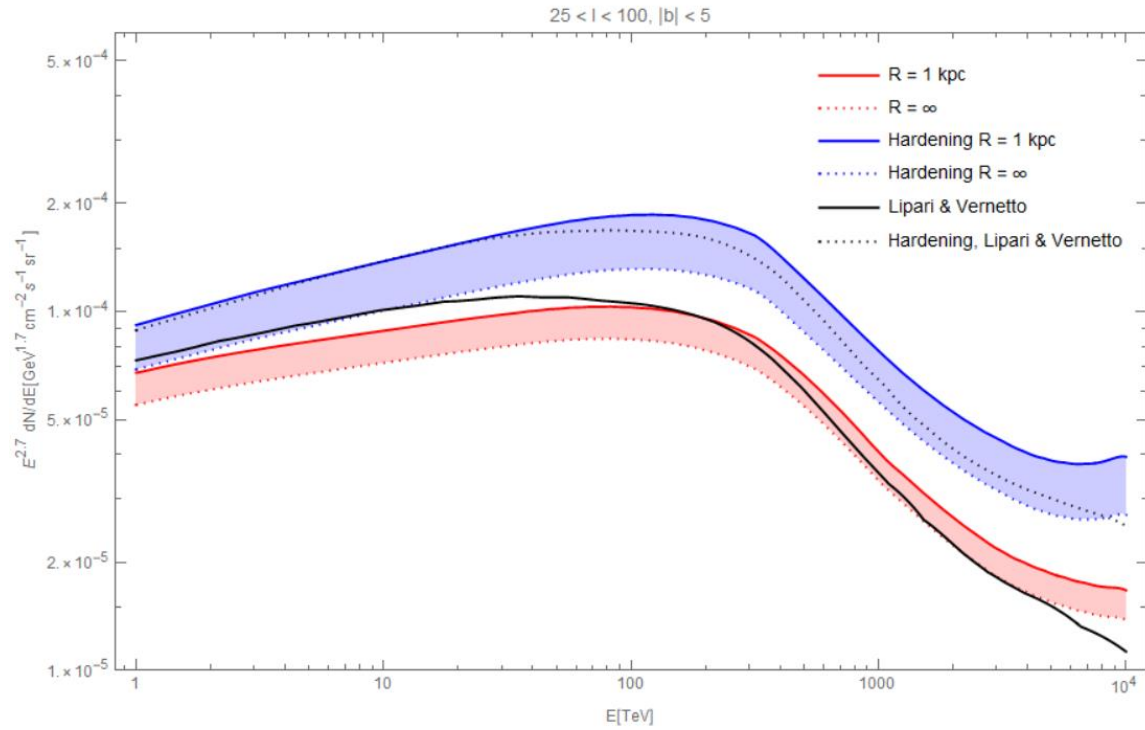
Why not LHAASO?

Extraction of Resolved Sources

Region:
Inner Galactic Plane
($25° < l < 100°$)

Masked radius $R < 2\sqrt{\text{p.s.f}^2 + \sigma_{ext}^2}$ $\sim 1°$

LHAASO Collaboration– ICRC 2021

Preliminary
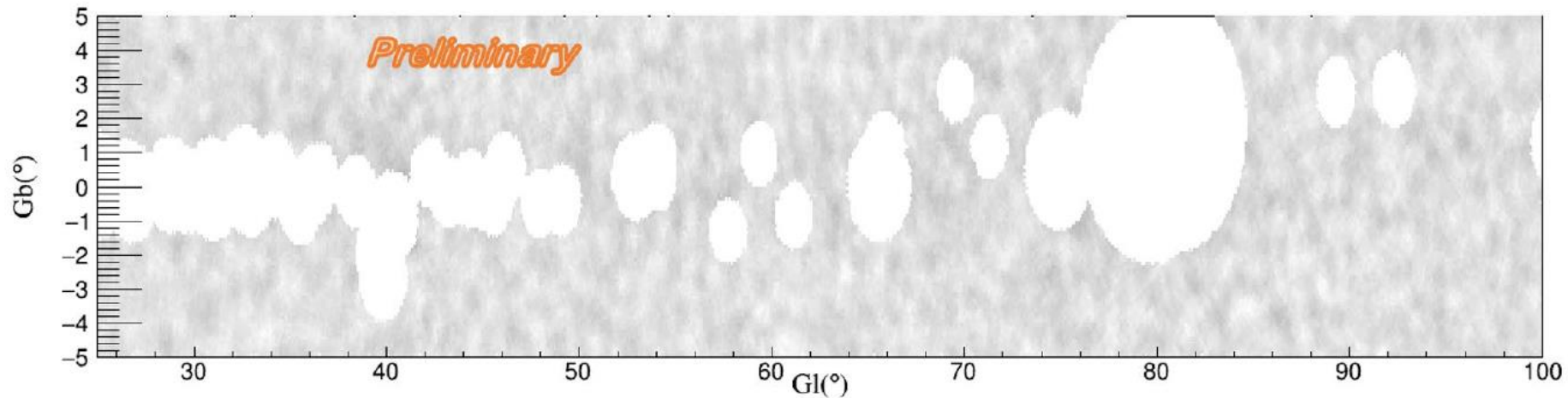
Cosmic ray local spectrum:

[*Dembinski, Engel, Fedynitch et al. (2018)*]
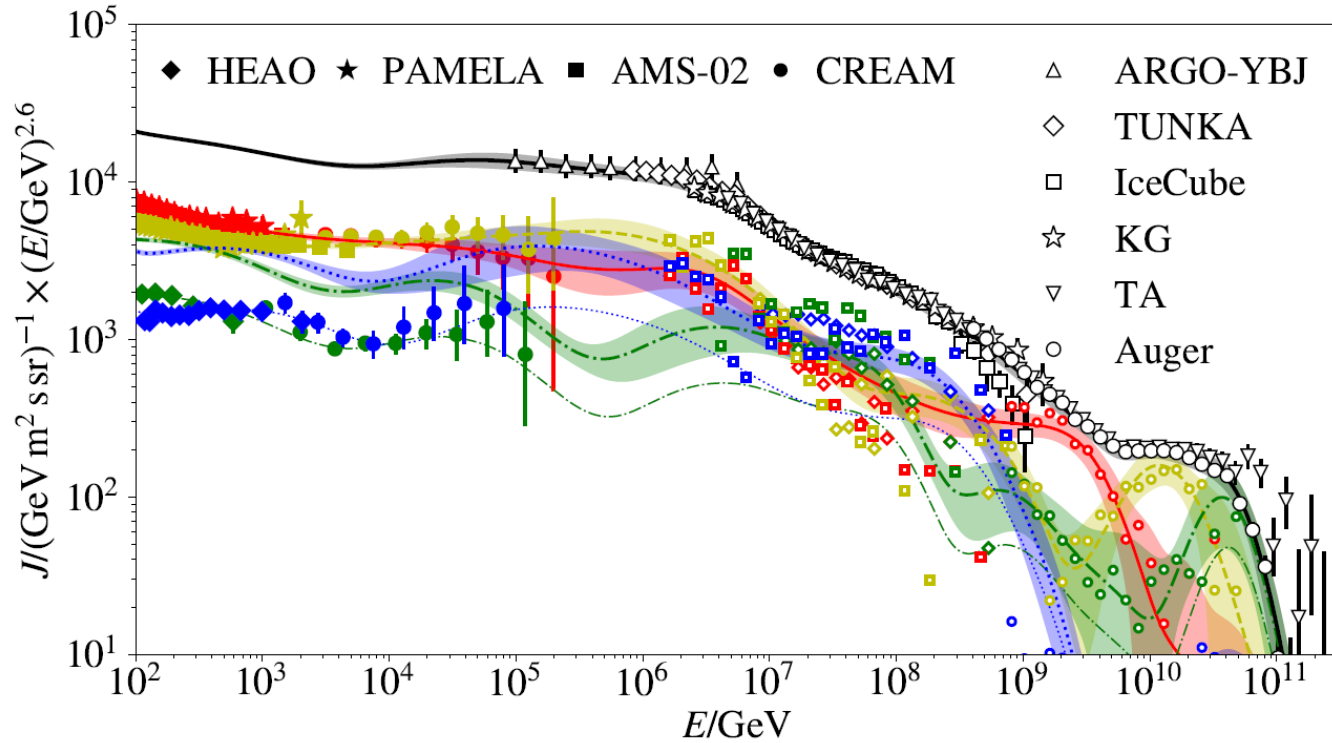
CR nucleons spectrum
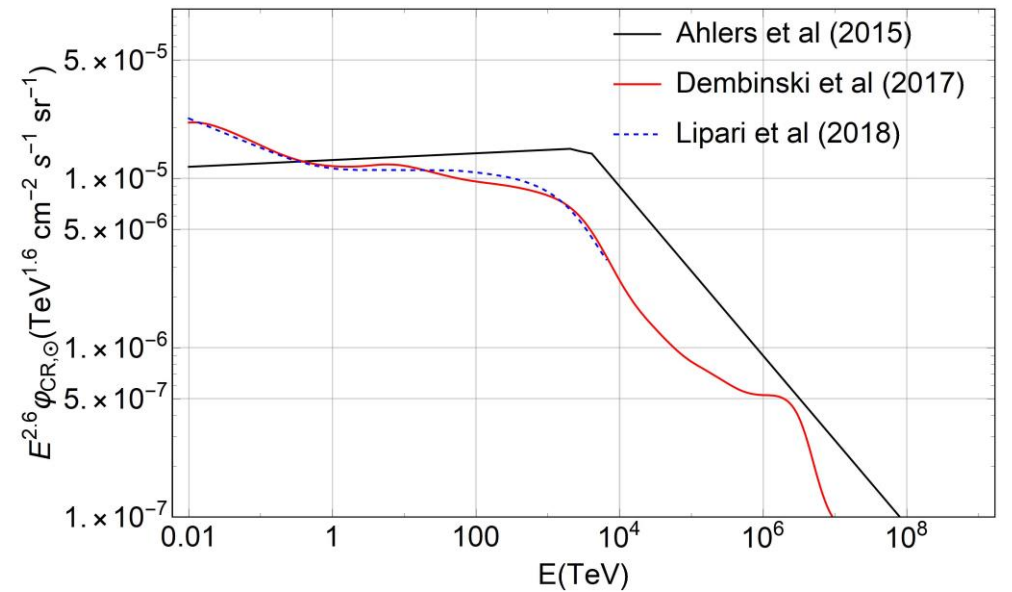
Cosmic ray distribution: 2 standard cases:

The function g(r) is determined by the distribution of the CR sources $f_s\,(\vec{r})$, that is assumed to follow the SNR number density parametrization given by Green et al. (2015), and by the propagation of CR in the Galactic magnetic field.

$$\varphi_{CR}(E, \vec{r}) = \varphi_{CR,Sun}(E)\, g\,(\vec{r}, R)$$

$$\begin{cases} R = 1\ kpc \\ R = \infty \end{cases}$$

Diffusion (smearing) radius

Data driven local CR spectrum [*Dembinski, Engel, Fedynitch et al. (2018)*]

SNR distribution [Green *et Al.* *(2015)*]

R = 1 kpc

R = ∞

Galprop [*Strong et Al. (2004)*]

- Acero et al. 2016
- Yang et al. 2016
- Gaggero et al. 2018
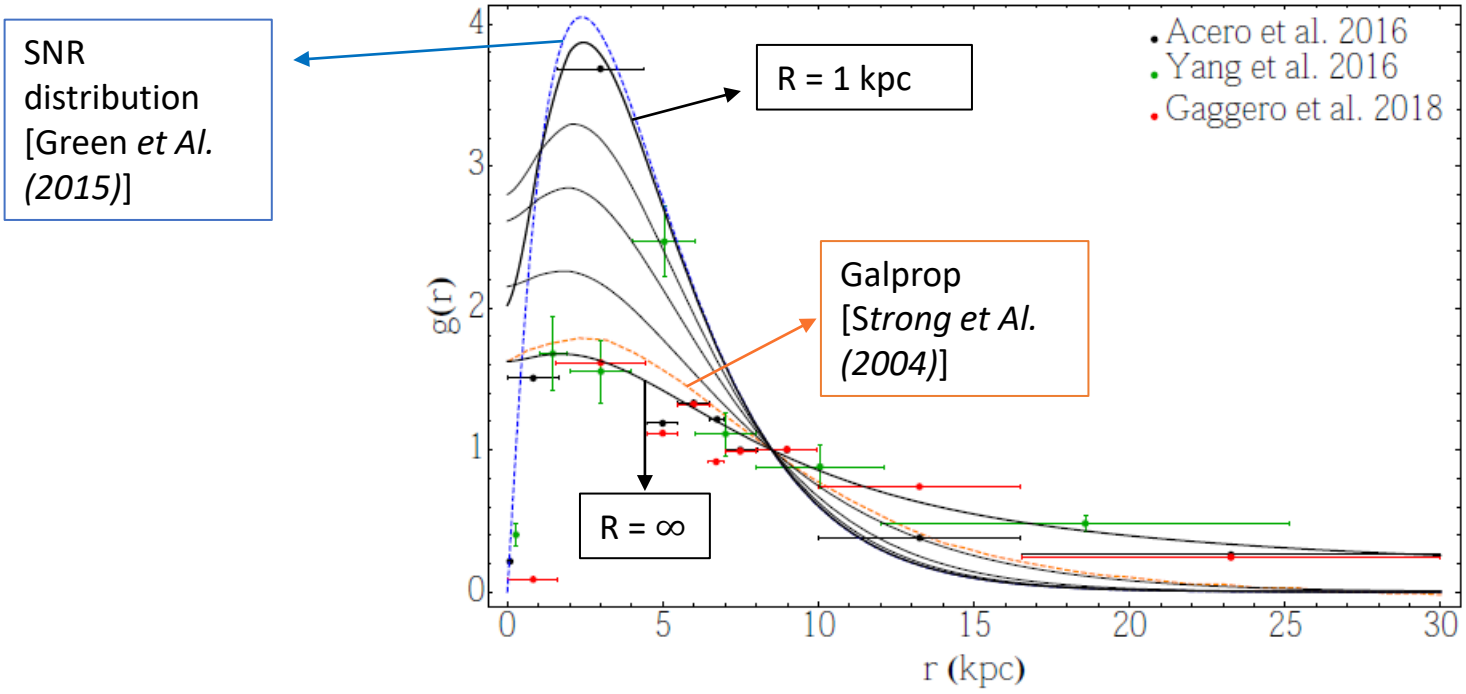
Cosmic ray distribution: 2 cases with hardening:

We consider the possibility of spatially dependent CR spectral index recenty emerged from the analysis of the FermiLAT data at $\sim 20\ GeV$ [*Acero et al. (2016), Yang et al. (2016), Gaggero et al. (2018)*]

$$\varphi_{CR}(E, \vec{r}) = \varphi_{CR,Sun}(E)\, g\,(\vec{r}, R)\, h(E, \vec{r})$$

$$\begin{cases} R = 1\ kpc \\ R = \infty \end{cases}$$
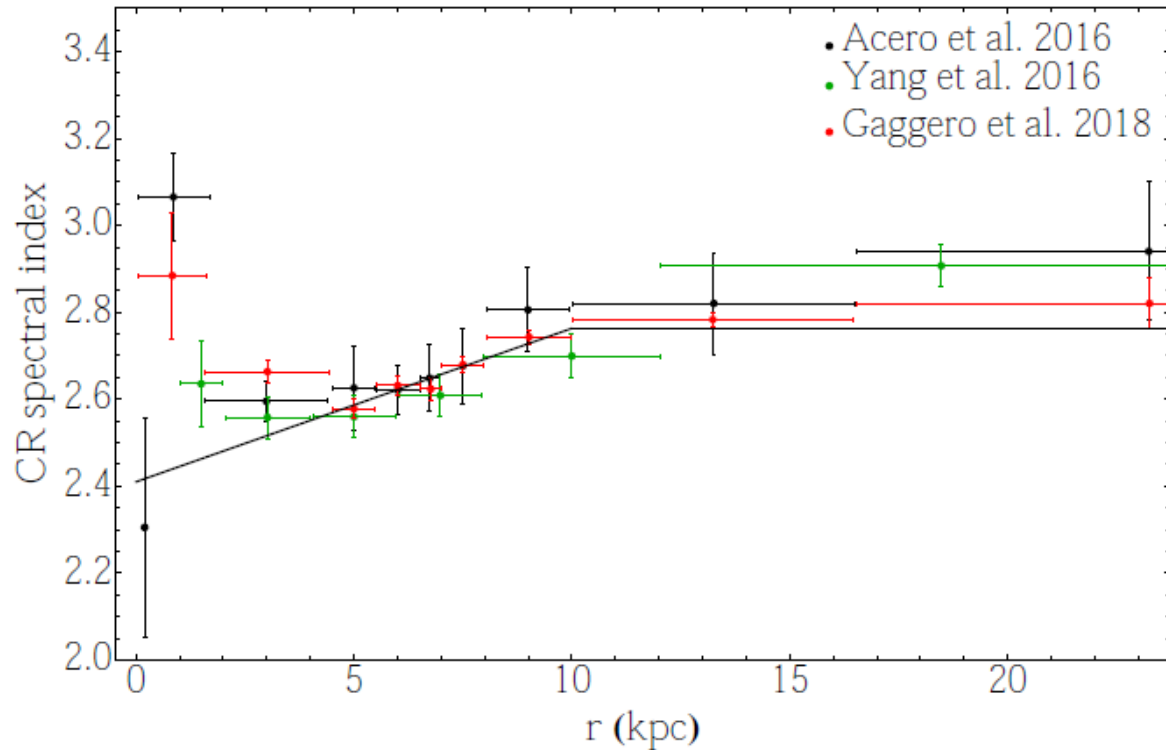
$$h(E, \vec{r}) = \left(\frac{E}{20\ GeV} \right)^{\Delta(\vec{r})}$$

$$\Delta(\vec{r}, z) = 0.3\left(1 - \frac{r}{r_{sun}}\right) \text{ for } r < 10 \text{ kpc}$$
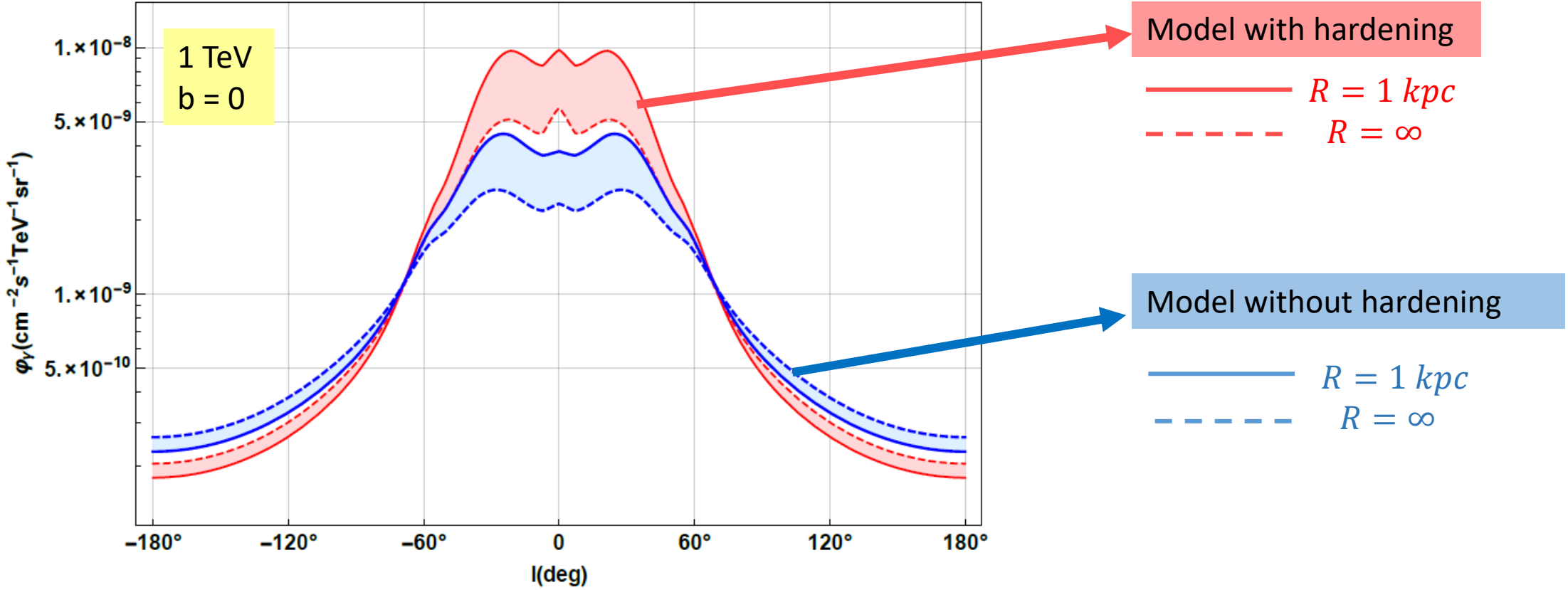
Diffuse Galactic gamma-ray emission:

Model: The power-law for the luminosity distribution can be automatically obtained assuming a fading source population (like PWNe, TeV Halos) create at a constant rate $\bar{r}$.

The spin-down power is described by: $\dot{E}(t) = \dot{E}_0 \left(1 + \dfrac{t}{\tau}\right)^{-2}$

Considering that a fraction $\lambda(t)$ of the spin-down power is converted into gamma-rays then the intrinsic luminosity decreases according to:

$$L(t) = \lambda(t)\dot{E}(t) = \underset{L_{max}}{\lambda\dot{E}_0}\left(1 + \dfrac{t}{\tau}\right)^{-\gamma} \text{where } \gamma = 2(\delta + 1);$$

$$\lambda(t) = \lambda \left(\dfrac{\dot{E}(t)}{\dot{E}_0}\right)^{\delta}$$

Abdalla et al, *A&A*, 612, A2 (2018)

Then:

$$Y(L) = \dfrac{\overline{r}\, \tau\, (\alpha - 1)}{L_{max}}\left(\dfrac{L}{L_{max}}\right)^{-\alpha}$$

Where $\bar{r} = 0.019\ yr^{-1}$ is the SN's rate and $\alpha = \left(\dfrac{1}{\gamma} + 1\right)$ therefore for $\gamma = 2$ we have $\alpha = 1.5$.

And instead of the parameter N we have the spin-down timescale of the Pulsar τ.

G S
S I

37

Model: The power-law for the luminosity distribution can be automatically obtained assuming a fading source population (like PWNe, TeV Halos) create at a constant rate $\bar{r}$.

The spin-down power is described by: $\dot{E}(t) = \dot{E}_0 \left(1 + \frac{t}{\tau}\right)^{-\frac{n+1}{n-1}}$

Considering that a fraction $\lambda(t)$ of the spin-down power is converted into gamma-rays then the intrinsic luminosity decreases according to:

$$L(t) = \lambda(t)\dot{E}(t) = \underset{L_{max}}{\lambda\dot{E}_0}\left(1 + \frac{t}{\tau}\right)^{-\gamma} \text{ where } \gamma = -\frac{n+1}{n-1}(\delta + 1);$$

$$\lambda(t) = \lambda\left(\frac{\dot{E}(t)}{\dot{E}_0}\right)^{\delta}$$

Abdalla et al, *A&A*, 612, A2 (2018)

Then:

$$Y(L) = \frac{\bar{r}\,\tau\,(\alpha - 1)}{L_{max}}\left(\frac{L}{L_{max}}\right)^{-\alpha}$$

Where $\bar{r} = 0.019\ yr^{-1}$ is the SN's rate and $\alpha = \left(\frac{1}{\gamma} + 1\right)$ therefore for $\gamma = 2$ we have $\alpha = 1.5$.

And instead of the parameter N we have the spin-down timescale of the Pulsar τ.

Results:

Best fit values for the reference case:

$$L_{\max} = 4.9^{+3.0}_{-2.1} \times 10^{35} \text{ergs/s}$$

$$\mathcal{N} = 17^{+14}_{-6}$$

all possible best fit values

$N = N_{obs}$

$L_{MW, Best Fit}$

$\mathcal{N}$

$L_{\max} / (10^{35} \text{ erg s}^{-1})$

$L_{max} \to \infty$
$L_{max} \to 0$
$L_{max} = L_{bf}$
$L_{max} = 2.3 L_{bf}$

$\propto \phi^{-\frac{3}{2}}$

$N = N_{obs}$

$\propto \phi^{1-\alpha}$

\#Sources >Flux

Flux>1 TeV(% Crab)
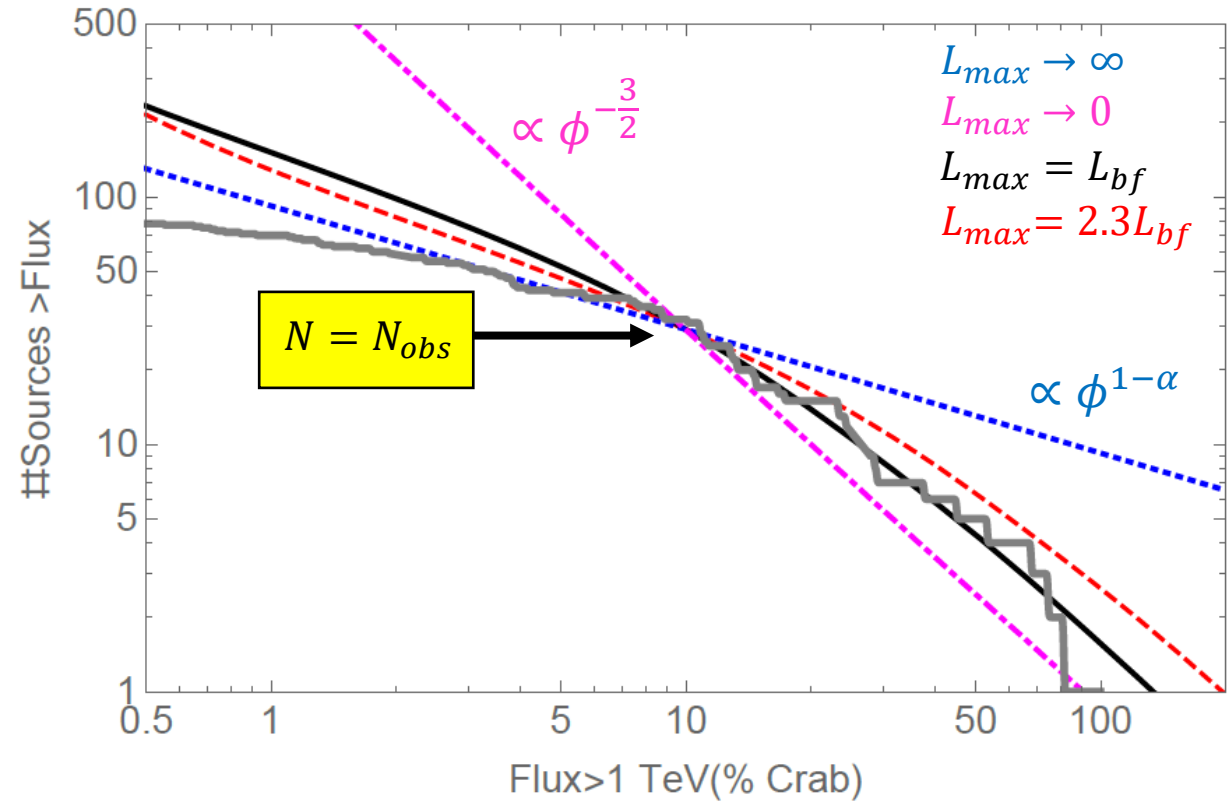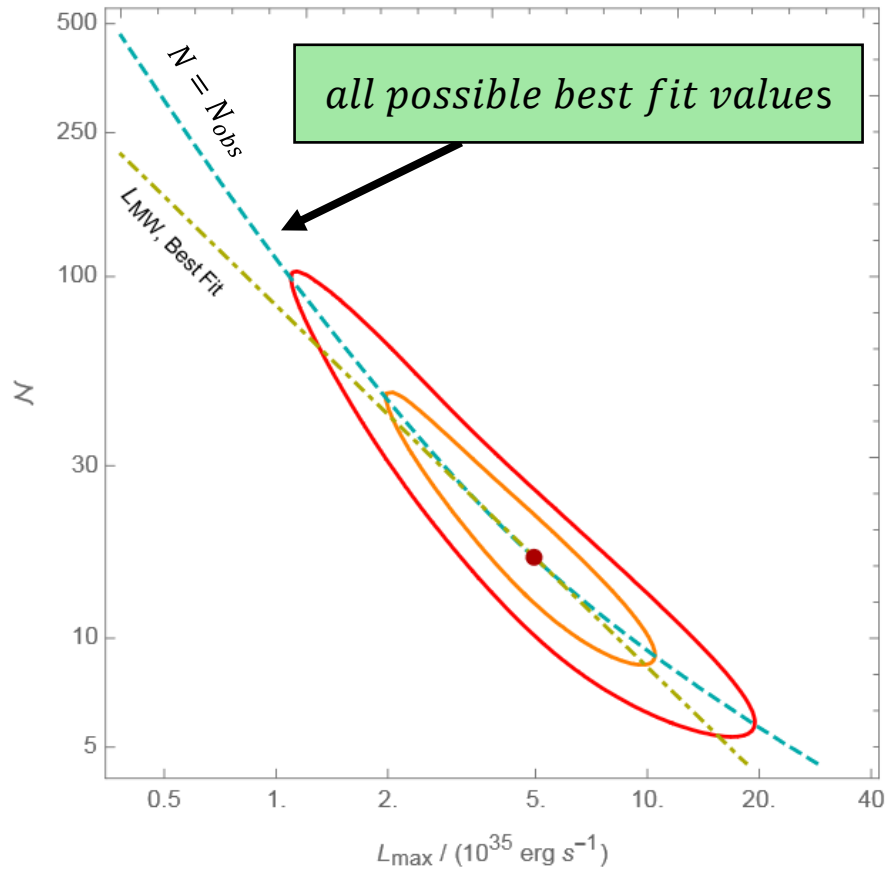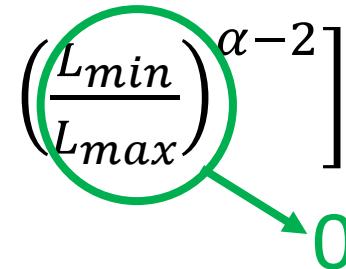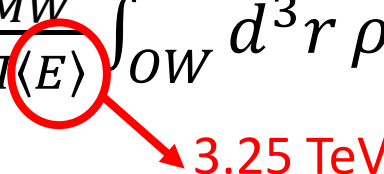
Results:

- The total TeV luminosity (1-100 TeV) of the Galaxy:

$$L_{MW} = \frac{N\,L_{max}}{(2-\alpha)}\left[1 - \left(\frac{L_{min}}{L_{max}}\right)^{\alpha-2}\right] = 1.7^{+0.5}_{-0.4} \times 10^{37}\ erg\ \text{s}^{-1}$$

0

- The flux at Earth produced by all sources (1-100 TeV) (resolved and unresolved) in the H.E.S.S. OW:

$$\phi_{tot} = \frac{L_{MW}}{4\Pi\langle E\rangle}\int_{OW} d^3r\,\rho(r)r^{-2} = 3.8^{+1.0}_{-1.0} \times 10^{-10}cm^{-2}s^{-1}$$

3.25 TeV

- By subtraction we can obtain the contribution of unresolved sources in the H.E.S.S. observational window knowing that: $\phi_{S,res} = 2.3 \times 10^{-10}cm^{-2}s^{-1}$ (cumulative flux due to all 78 sources):

$$\boxed{\phi_{S,unres} = \phi_{tot} - \phi_{S,res} = 1.4^{+1.0}_{-0.8} \times 10^{-10}\ cm^{-2}s^{-1}} \sim 60\%\ \phi_{S,res} \sim 30\%\ \phi_{tot}$$

Robustness of the results:

	$\log_{10}\frac{L_{\max}}{\mathrm{erg\,s}^{-1}}$	$\mathcal{N}$	$\log_{10}\frac{L_{\mathrm{MW}}}{\mathrm{erg\ s}^{-1}}$	Φ_{tot}	τ	$\Delta\chi^2$
Ref.	$35.69^{+0.21}_{-0.28}$	17^{+14}_{-6}	$37.22^{+0.12}_{-0.13}$	$3.8^{+1.0}_{-1.0}$	$1.8^{+1.5}_{-0.6}$	–
SNR	$35.69^{+0.22}_{-0.25}$	18^{+15}_{-7}	$37.23^{+0.12}_{-0.13}$	$3.8^{+1.0}_{-1.0}$	$1.8^{+1.6}_{-0.7}$	1.4
$H = 0.1\,\mathrm{kpc}$	$35.65^{+0.22}_{-0.27}$	$15^{+14.5}_{-6}$	$37.13^{+0.12}_{-0.13}$	$5.0^{+0.4}_{-2.0}$	$1.6^{+1.5}_{-0.6}$	-7.3
$H = 0.05\,\mathrm{kpc}$	$35.34^{+0.26}_{-0.19}$	28^{+19}_{-13}	$37.08^{+0.12}_{-0.13}$	$4.4^{+1.3}_{-0.9}$	$2.9^{+2.0}_{-1.4}$	-10.5
$d = 20\,\mathrm{pc}$	$35.69^{+0.20}_{-0.26}$	17^{+16}_{-6}	$37.23^{+0.12}_{-0.13}$	$3.9^{+0.8}_{-1.0}$	$1.9^{+1.9}_{-0.7}$	-0.2
$d = 40\,\mathrm{pc}$	$35.67^{+0.20}_{-0.25}$	20^{+20}_{-8}	$37.28^{+0.12}_{-0.13}$	$4.4^{+1.2}_{-1.1}$	$2.2^{+2.0}_{-0.8}$	-1.8
$\alpha = 1.3$	$35.61^{+0.18}_{-0.27}$	$25^{+24}_{-8.5}$	$37.17^{+0.12}_{-0.13}$	$3.5^{+1.1}_{-0.9}$	$4.3^{+4.3}_{-1.5}$	0.0
$\alpha = 1.8$	$35.83^{+0.29}_{-0.24}$	7^{+6}_{-4}	$37.39^{+0.11}_{-0.13}$	$5.9^{+1.8}_{-0.1}$	$0.5^{+0.4}_{-0.2}$	0.5

Robustness of the results:

	$\log_{10} \frac{L_{\max}}{\text{erg s}^{-1}}$	$\mathcal{N}$	$\log_{10} \frac{L_{\text{MW}}}{\text{erg s}^{-1}}$	Φ_{tot}	τ	$\Delta\chi^2$
Ref.	$35.69^{+0.21}_{-0.28}$	17^{+14}_{-6}	$37.22^{+0.12}_{-0.13}$	$3.8^{+1.0}_{-1.0}$	$1.8^{+1.5}_{-0.6}$	—
SNR	$35.69^{+0.22}_{-0.25}$	18^{+15}_{-7}	$37.23^{+0.12}_{-0.13}$	$3.8^{+1.0}_{-1.0}$	$1.8^{+1.6}_{-0.7}$	1.4
$H = 0.1\,\text{kpc}$	$35.65^{+0.22}_{-0.27}$	$15^{+14.5}_{-6}$	$37.13^{+0.12}_{-0.13}$	$5.0^{+0.4}_{-2.0}$	$1.6^{+1.5}_{-0.6}$	-7.3
$H = 0.05\,\text{kpc}$	$35.34^{+0.26}_{-0.19}$	28^{+19}_{-13}	$37.08^{+0.12}_{-0.13}$	$4.4^{+1.3}_{-0.9}$	$2.9^{+2.0}_{-1.4}$	-10.5
$d = 20\,\text{pc}$	$35.69^{+0.20}_{-0.26}$	17^{+16}_{-6}	$37.23^{+0.12}_{-0.13}$	$3.9^{+0.8}_{-1.0}$	$1.9^{+1.9}_{-0.7}$	-0.2
$d = 40\,\text{pc}$	$35.67^{+0.20}_{-0.25}$	20^{+20}_{-8}	$37.28^{+0.12}_{-0.13}$	$4.4^{+1.2}_{-1.1}$	$2.2^{+2.0}_{-0.8}$	-1.8
$\alpha = 1.3$	$35.61^{+0.18}_{-0.27}$	$25^{+24}_{-8.5}$	$37.17^{+0.12}_{-0.13}$	$3.5^{+1.1}_{-0.9}$	$4.3^{+4.3}_{-1.5}$	0.0
$\alpha = 1.8$	$35.83^{+0.29}_{-0.24}$	7^{+6}_{-4}	$37.39^{+0.11}_{-0.13}$	$5.9^{+1.8}_{-0.1}$	$0.5^{+0.4}_{-0.2}$	0.5

The quality of the fit improves by reducing the thickness of the disk.

Robustness of the results:

	$\log_{10} \frac{L_{\max}}{\mathrm{erg\,s^{-1}}}$	$\mathcal{N}$	$\log_{10} \frac{L_{MW}}{\mathrm{erg\ s^{-1}}}$	Φ_{tot}	τ	$\Delta\chi^2$
Ref.	$35.69^{+0.21}_{-0.28}$	17^{+14}_{-6}	$37.22^{+0.12}_{-0.13}$	$3.8^{+1.0}_{-1.0}$	$1.8^{+1.5}_{-0.6}$	$-$
SNR	$35.69^{+0.22}_{-0.25}$	18^{+15}_{-7}	$37.23^{+0.12}_{-0.13}$	$3.8^{+1.0}_{-1.0}$	$1.8^{+1.6}_{-0.7}$	1.4
$H = 0.1\,\mathrm{kpc}$	$35.65^{+0.22}_{-0.27}$	$15^{+14.5}_{-6}$	$37.13^{+0.12}_{-0.13}$	$5.0^{+0.4}_{-2.0}$	$1.6^{+1.5}_{-0.6}$	-7.3
$H = 0.05\,\mathrm{kpc}$	$35.34^{+0.26}_{-0.19}$	28^{+19}_{-13}	$37.08^{+0.12}_{-0.13}$	$4.4^{+1.3}_{-0.9}$	$2.9^{+2.0}_{-1.4}$	-10.5
$d = 20\,\mathrm{pc}$	$35.69^{+0.20}_{-0.26}$	17^{+16}_{-6}	$37.23^{+0.12}_{-0.13}$	$3.9^{+0.8}_{-1.0}$	$1.9^{+1.9}_{-0.7}$	-0.2
$d = 40\,\mathrm{pc}$	$35.67^{+0.20}_{-0.25}$	20^{+20}_{-8}	$37.28^{+0.12}_{-0.13}$	$4.4^{+1.2}_{-1.1}$	$2.2^{+2.0}_{-0.8}$	-1.8
$\alpha = 1.3$	$35.61^{+0.18}_{-0.27}$	$25^{+24}_{-8.5}$	$37.17^{+0.12}_{-0.13}$	$3.5^{+1.1}_{-0.9}$	$4.3^{+4.3}_{-1.5}$	0.0
$\alpha = 1.8$	$35.83^{+0.29}_{-0.24}$	7^{+6}_{-4}	$37.39^{+0.11}_{-0.13}$	$5.9^{+1.8}_{-0.1}$	$0.5^{+0.4}_{-0.2}$	0.5

$$L_{MW} = (1.2 - 2.5) \times 10^{37}\ erg\ s^{-1}$$

$$\phi_{tot} = (3.5 - 5.9)10^{-10} cm^{-2} s^{-1}$$

Likelihood:

$$\log L = -\mu_{tot} + \sum_i \log(\mu_i)$$

- μ_{tot} represents the number of expected sources;
- μ_i is the probability to observe an object with coordinates (b_i, l_i) and measured flux ϕ_i.

The source distribution per unit of flux is:

$$\mu(b, l, \phi) = \int dr \, 4\pi r^4 \rho(r, l, b) Y(4\pi r^2 \langle E \rangle \phi)$$

While is given by:

$$\mu_i = \int d\phi \mu(b_i, l_i, \phi_i) P(\phi_i, \phi, \delta\phi_i)$$

Where $P(\phi_i, \phi, \delta\phi_i)$ respresents the probability that the measured flux ϕ_i is obtained for the real flux ϕ.
We assume a Gaussian.
The $\chi^2 = -2logL$ was used for obtaining the best fit values and the allowed regions for the parameters.

Cumulative distribution:

The flux distribution can be calculated as:

$$\frac{dN}{d\Phi} = \int dr \; 4\pi r^4 \langle E \rangle \; Y(4\pi r^2 \langle E \rangle \Phi) \; \overline{\rho}(r)$$

- $\overline{\rho}(r)$ is the sources spatial distribution integrated over the longitude and latitude intervals probed by H.E.S.S.;
- The above integral is performed in the range $d/\theta_{max} \leq r \leq D(L,\phi) =$ where $\theta_{max} = 0.7^o$ is the maximal angular dimension that can be probed by H.E.S.S. and the d is the physical dimention of the source. While $D(L,\phi) = (L/4\,\pi\,\langle E \rangle\,\phi)^{\frac{1}{2}}$;

- We calculate analytically the flux distribution for the 2 limits cases $L_{max} \rightarrow \infty$ and $L_{max} \rightarrow 0$:

$$\frac{dN}{d\Phi} = R\,\tau\,(\alpha - 1)\,L_{\max}^{\alpha-1}\,\Phi^{-\alpha} \int_0^\infty dr \; (4\pi\langle E \rangle)^{1-\alpha}\,r^{4-2\alpha}\,\overline{\rho}(r)$$

$$\frac{dN}{d\Phi} \simeq (4\pi\langle E \rangle)^{1-\alpha}\,\overline{\rho}(0)\,R\,\tau\,(\alpha - 1)\,L_{\max}^{\alpha-1}\,\Phi^{-\alpha} \int_0^{D(L_{\max},\Phi)} dr \; r^{4-2\alpha} = \overline{\rho}(0)\,R\,\tau\left(\frac{\alpha - 1}{5 - 2\alpha}\right)\left(\frac{L_{\max}}{4\pi\langle E \rangle}\right)^{\frac{3}{2}}\Phi^{-\frac{5}{2}}$$

45

Resolved and Unresolved sources:

The resolved flux can be calculated from:

$$\phi_{res} = \int dr \; r^2 \bar{\rho}(r) \int d\phi \; 4\pi \langle E \rangle r^2 \phi \; Y(4\pi r^2 \langle E \rangle \phi)$$

$$\phi_{res} = \int dr \; \bar{\rho}(r) \int dL \frac{L}{4\,\pi\,\langle E \rangle} Y(L)$$

$$\phi_{res} = \phi_{th} \int dr \bar{\rho}(r) \int dL \bar{D}(L)^2 Y(L)$$

- $\bar{\rho}(r)$ is the sources spatial distribution integrated over the longitude and latitude intervals probed by H.E.S.S.;
- The above integral is performed in the range $d/\theta_{max} \leq r \leq D(L,\phi)$ where $\theta_{max} = 0.7^o$ is the maximal angular dimension that can be probed by H.E.S.S. and the d is the physical dimention of the source. While $D(L,\phi) = (L/4\pi\langle E\rangle\phi)^{\frac{1}{2}}$;
- The luminosity integral is performed in the range $L_{min}(r) \leq L \leq L_{max}$ where $L_{min} = 4\pi r^2 \langle E \rangle \phi_{th}$

$$=$$